Beyond Ice

NASA's ICESat-2 spaceborne lidar mission for land and vegetation applications

©SHUTTERSTOCK.COM/MIHA CREATIVE

CARLOS ALBERTO SILVA, AMY NEUENSCHWANDER, CAIO HAMAMURA, SÉRGIO GODINHO, KODY M. BROCK, LONESOME MALAMBO, LANA NARINE, JEFF W. ATKINS, JORDAN S. BORAK, SORIN POPESCU, INACIO T. BUENO, LUCAS BIELAK REZENDE, GIULIO BROSSI SANTORO, ANA PAULA DALLA CORTE, CESAR IVAN ALVITES DIAZ, NOOSHIN MASHHADI, ADRIÁN CARDIL, ANDREW T. HUDAK, LAURI KORHONEN, AJAY SHARMA, JEFFERY B. CANNON, MIDHUN MOHAN, WAN SHAFRINA WAN MOHD JAAFAR, VERALDO LIESENBERG, AND CARINE KLAUBERG

The extension of NASA's Ice, Cloud, and land Elevation Satellite-2 (ICESat-2) mission beyond the cryosphere to include the study of vegetation and the land surface has significantly advanced global Earth observation. This review synthesizes findings from 293 peer-reviewed articles and provides a comprehensive assessment of the mission's contributions to terrestrial ecosystem science. We begin by outlining the mission's objectives, instrumentation, and core data products—particularly ATL03 (geolocated photons) and ATL08 (terrain and canopy heights)—which have supported a wide array of applications in forestry, terrain analysis, and environmental monitoring. Our analysis shows that most studies focus on temperate and tropical broadleaf forests, with a strong emphasis on estimating canopy height, terrain elevation, and forest structure. Terrain metrics derived from *ICESat-2* products typically achieve high accuracy, while vegetation variables, such as canopy height, cover, leaf area index (LAI), and aboveground biomass, demonstrate moderate to strong accuracies across biomes. While parametric models remain the most used approach, machine learning methods are expanding, and more than one third of the reviewed literature incorporates synergistic analyses with other satellite missions. Despite its versatility, *ICESat-2* remains underutilized in several key domains—including nonforest vegetation, fire ecology, wildlife habitat assessment, urban monitoring, and disturbance detection—mainly due to the scarcity of standardized algorithms and validated reference datasets. However, the growing availability of open source processing tools presents a significant opportunity for expanding the user base and fostering innovation in these

Digital Object Identifier 10.1109/MGRS.2026.3666794
Date of publication 10 March 2026; date of current version 5 June 2026.

emerging areas. Future advancements, such as the forthcoming ATL18 gridded canopy height and terrain products, alongside synergies with missions like the European Space Agency (ESA)'s BIOMASS and the NASA–Indian Space Research Organisation (ISRO) Synthetic Aperture Radar (NISAR), promise to enhance multisensor integration and ecosystem monitoring. Overall, *ICESat-2* continues to evolve as a powerful resource for characterizing vegetation structure, ecosystem dynamics, and land surface processes on a global scale.

INTRODUCTION

In the era of space-based observation, the advent of spaceborne lidar technologies, such as NASA's *ICESat-2*, has revolutionized our capacity to capture and interpret 3D ecosystem structure, which has profound implications for our understanding of the Earth system. *ICESat-2* was launched on 15 September 2018 with the primary objective of measuring the elevation of Earth's ice sheets, glaciers, and sea ice [1]. The ICESat-2 mission accomplishes this with the Advanced Topographic Laser Altimeter System (ATLAS), which emits laser pulses toward Earth's surface, accurately timing their return to calculate elevation [2]. While the primary goal of the ICESat-2 mission is to monitor changes in the cryosphere, the geodetic measurements the satellite collects over Earth's terrestrial surface have a wide range of terrestrial applications [3].

ICESat-2 provides precise 3D representations of Earth's surface within latitudes ranging from 88° S to 88° N (Figure 1; [2]). Two of the mission's data products, ATL08 (terrain and canopy heights) and the forthcoming ATL18 (gridded canopy height and terrain), are tailored to meet the specific requirements of land and vegetation applications. In alignment with the mission's scientific mandate concerning terrestrial ecosystems, *ICESat-2* is engineered to deliver accurate, geolocated canopy and terrain height measurements allowing for global estimates of canopy height [1]. This accuracy is facilitated through an equatorial ground track spacing of less than 2 km that is expected to decrease as new data are acquired beyond the primary three-year mission [1]. The data acquisition strategy employed by *ICESat-2* is designed to permit comprehensive surface height characterization over large geographic extents with global scalability potential [2], [4]. Such data have many applications for terrestrial ecosystem science, most notably in quantifying forest structure [5], [6], biomass mapping and monitoring [7], [8], [9], [10], and assessment of fire [11] and flooding disturbance [12].

MOST STUDIES FOCUS ON TEMPERATE AND TROPICAL BROADLEAF FORESTS, WITH A STRONG EMPHASIS ON ESTIMATING CANOPY HEIGHT, TERRAIN ELEVATION, AND FOREST STRUCTURE.

Despite a growing emphasis on the use of spaceborne lidar systems for land and vegetation applications [13], to

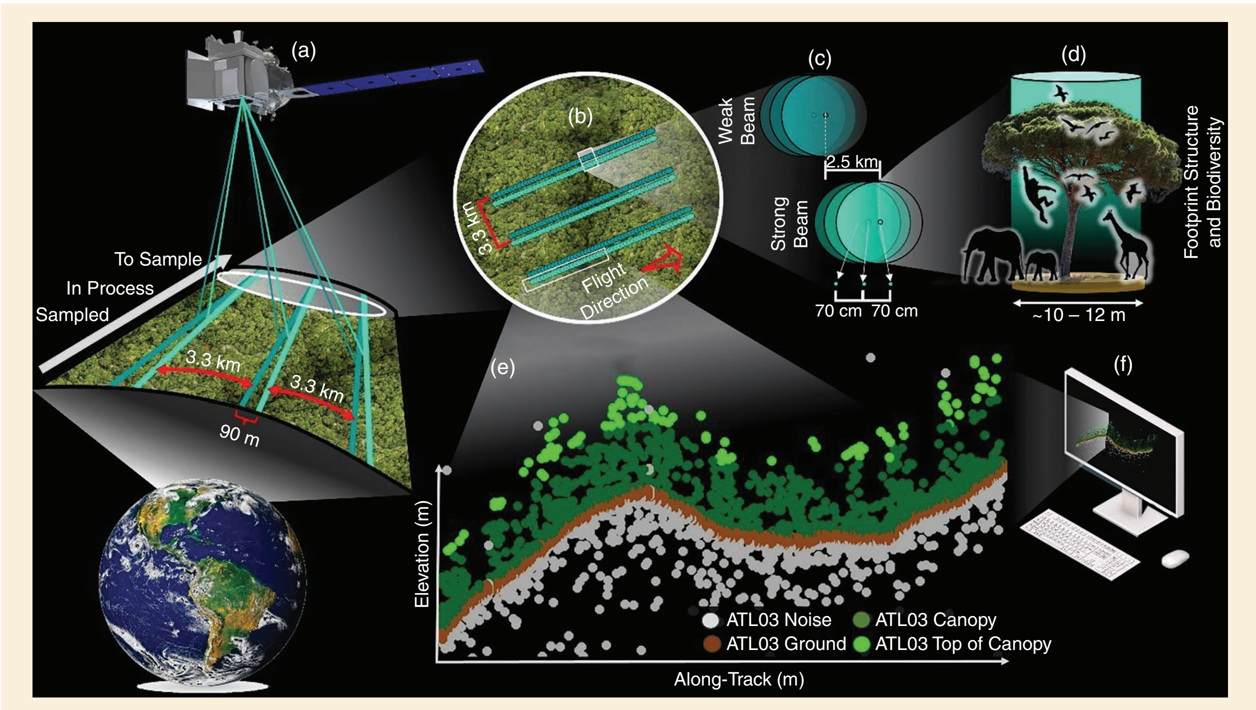

FIGURE 1. (a) ICESat-2 global coverage and sampling scheme. (b) Six beam patterns. (c) Laser beam distance along and between weak and strong tracks. (d) Laser beam footprint of ~10–12 m over a forested area. (e) ATL03 labeled photon cloud. (f) Analysis of ATL03 and ATL08 products.

date, only a few published review articles by the ICEsat-2 Science Team have highlighted the capabilities of the ICESat-2 mission for land and vegetation applications. One such article by Markus et al. [1] provided a preview of the ICESat-2 mission and its scientific goals and objectives. Magruder et al. [4] provided an early, postlaunch mission synopsis and observatory performance of *ICESat-2*, while Neumann et al. [2] described the major components of ATLAS, including the transmitter, the receiver, and the components of the timing system. For land and vegetation applications, Neuenschwander and Pitts [3] provided a detailed description of the ATL08 methodology, data format, and products, such as terrain and canopy height estimates, and their respective uncertainties. More recently, Brown et al. [14] conducted a literature review of articles from 2013 to 2021 that included both *ICESat* [15] and *ICESat-2* data to identify relevant applications that could lead to the use of data products in decision making, policy making, or risk reduction activity for societal benefit. Although the review discussed the use of *ICESat-2* for terrestrial applications, it focused on general applications of *ICESat-2*. Therefore, limited information has been available on mission updates and improvements since its launch in 2018, and there is an increasing need for a comprehensive literature review of studies using *ICESat-2* for terrestrial applications.

TERRAIN METRICS DERIVED FROM *ICESAT-2* PRODUCTS TYPICALLY ACHIEVE HIGH ACCURACY, WHILE VEGETATION VARIABLES SUCH AS CANOPY HEIGHT, COVER, LEAF AREA INDEX, AND ABOVEGROUND BIOMASS DEMONSTRATE MODERATE TO STRONG ACCURACIES ACROSS BIOMES.

This review directly addresses the current gap by compiling and analyzing recent *ICESat-2* research, with a focus on methodological advances and future opportunities for terrestrial ecosystem studies. We provide a detailed overview of the NASA ICESat-2 mission, including its instrumentation, data collection, and mission objectives, with an emphasis on its relevance to land and vegetation applications. To further enhance the discovery of *ICESat-2* applications, we include a comprehensive literature review of published studies. Our main objectives are to

1) systematically review and analyze a broad spectrum of global studies that have used *ICESat-2* data for land and vegetation applications
2) characterize the geographical distribution, methodologies, and research outcomes of these studies
3) critically assess the capabilities and limitations of *ICESat-2* data for land and vegetation studies
4) identify gaps in the current state of research
5) propose avenues for future investigation and technological refinement.

Furthermore, this study seeks to shed light on the future of this mission and its synergies with current and upcoming missions focused on terrestrial applications, such as NASA's Global Ecosystem Dynamics Investigation (GEDI) spaceborne lidar [16], NISAR [17], and the ESA's BIOMASS [18] missions. The study is organized as follows. In the next section, ICESat-2 mission objectives, requirements, and technical specifications are discussed. The section "Tools" explores the available stand-alone tools and new cloud computing capabilities for *ICESat-2* data processing and analysis. The section "Literature Review on *ICESat-2* for Terrestrial Applications" focuses on the comprehensive literature review on *ICESat-2* for terrestrial applications. The section "Discussion" discusses current limitations, future development, and new capabilities of *ICESat-2* for terrestrial application, the synergies to current and upcoming spaceborne missions, and also the gaps and topics for future research. In the final section, the conclusions are presented.

NASA'S ICESAT-2 MISSION

MISSION OBJECTIVES, DATA, PRODUCTS, AND REQUIREMENTS

ICESat-2's initial three-year mission, spanning from 14 October 2018 to 14 October 2021, focused primarily on measuring changes of land and sea ice elevations and extent to better understand the linkages to sea level rise and climate change. *ICESat-2* collects raw photon-counting lidar data using ATLAS, and these data are processed into standardized data products (Figure 2). These primary science objectives informed mission requirements for the vertical and horizontal accuracy and precision of height measurements—including a requirement for pointing control of better than 45 m and geolocation knowledge better than 5 m; however, recent validation calculations for Release 006 of the data indicate that these accuracies are ~3 m and 2.1 m [19], respectively. There is, however, ambiguity of the photon geolocation within the footprint diameter, meaning the true position of a photon could be reflected from anywhere within the laser footprint. The addition of a science objective to measure vegetation height as a basis for estimating biomass and biomass change [2] led to a mission requirement of collecting measurements in the nonpolar regions such that the spatial sampling was less than 2 km between tracks at the equator after two years. During the prime mission, *ICESat-2* data have demonstrated unprecedented spatial detail in height profiles over a variety of surfaces, including ice shelves (rifts, ice fronts, grounding zones, basal channels, and melt water depth), sea ice, the ocean (near-shore bathymetry and ocean surface topography) and vegetated land (forest canopy height and topography). Although there was no formal mission requirement regarding the accuracy of the estimated terrain and canopy heights, this study will illustrate the strengths and limitations of utilizing *ICESat-2* heights for terrestrial ecosystems.

ORBITS, POINTING STRATEGY, MAPS OF COVERAGE DENSITY

The *ICESat-2* satellite was placed into a 454-km orbit with a 92° inclination, and it collects 1,387 reference orbits during a 91-day repeat orbit cycle to provide monthly, seasonal, and annual measurements in the polar areas. This orbit results in global coverage from 88° S to 88° N. In the midlatitudes (~60° S to ~70° N), the ICESat-2 Project Science Office implemented an off-nadir pointing plan with the intention of increasing the distribution of measurements across the surface to meet the mission requirement of spatial sampling for vegetation [1]. Thus, in the midlatitudes, *ICESat-2* is off-pointed a maximum of 1.8° from the reference ground track every 91 days rather than repeating the reference track coverage (Figure 3). As the satellite approaches a land region, it is transitioned from the repeat track to the designated pointing angle. The commissioning phase of the satellite occurred during the first 45 days, and during the first two 91-day cycles (cycle 1 and cycle 2) the Project Science Office was refining the pointing control, knowledge, and ranging calibrations of the instrument. Throughout the mission, the Project Science Office has improved the ranging and calibration associated with the measured heights for each release of

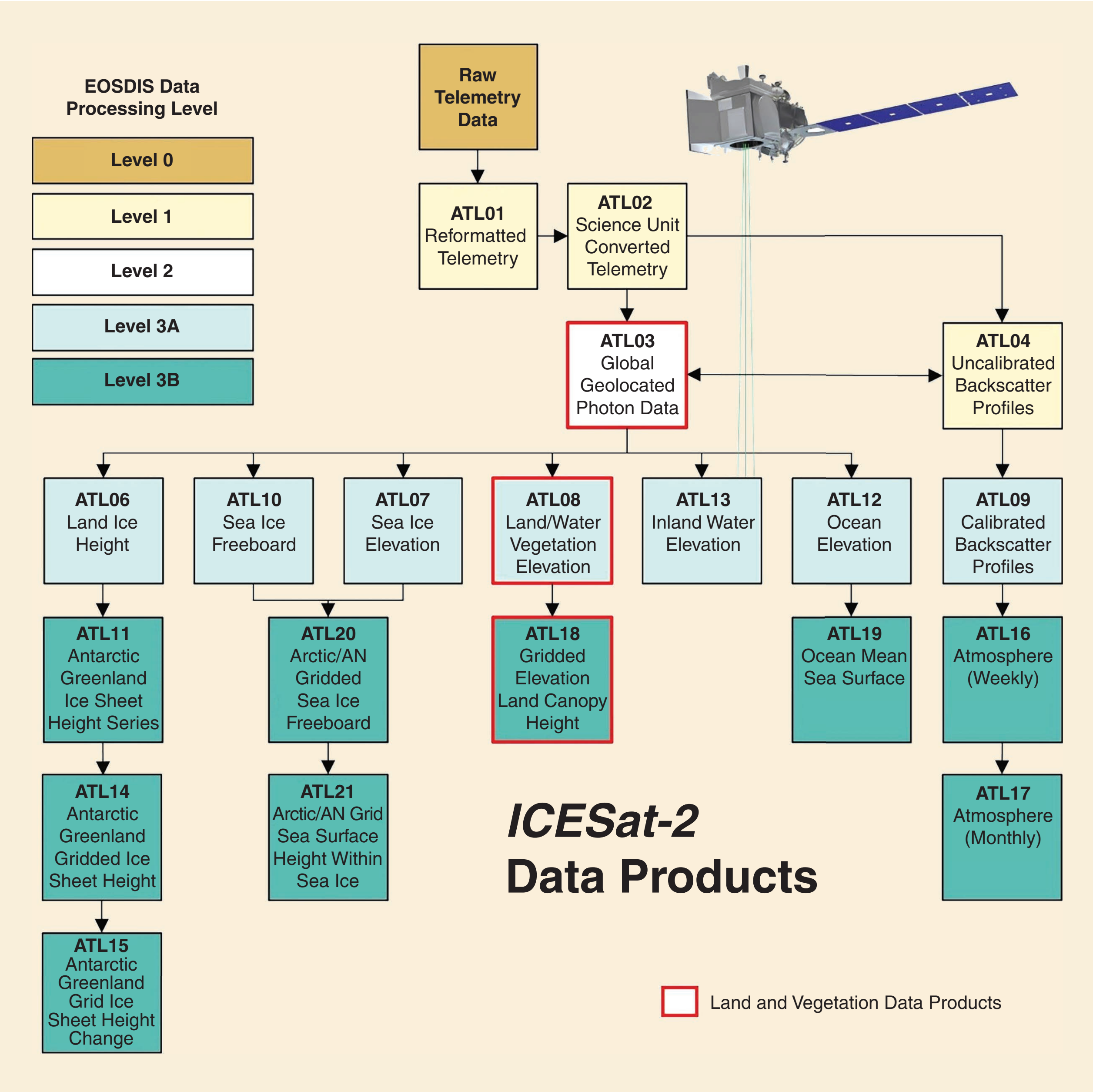

FIGURE 2. Illustration of the *ICESat-2* data products from NASA's EOSDIS: NASA's Earthdata, NSIDC DAAC). EOSDIS: Earth Observing System Data and Information System; NSIDC DAAC: National Snow and Ice Data Center Distributed Active Archive Center.

data. The off-nadir pointing plan during the prime mission officially commenced with cycle 3, which was the official first tracking of the reference ground tracks. The off-nadir pointing angles for each subsequent 91-day orbit cycle for the first seven years of the mission are provided in Figure 4. On 26 June 2019 (during cycle 4), as the solar panel was repositioning itself for optimal power, the voltage across the potentiometer was higher than expected, triggering an event. This event resulted in a satellite-issued command to power down the laser into "safehold mode" to prevent any damage to the instrument. A second safehold event for the same reason occurred on 4–11 April 2022. This first safehold event resulted in a three-week delay in collecting science data. Because of this delay, the pointing plan for cycle 4 was repeated in cycle 5.

Since the completion of the prime mission requirements, *ICESat-2* is currently operating under a modified pointing plan in the midlatitudes. It collects data along the reference ground tracks at snow-maximum and no-snow times in the Northern Hemisphere and continues to off-point the remaining cycles in an effort to allow for the estimation of snow depth and height changes of fast-moving glaciers. Cycles collected during the summer will be repeated with roughly two years between each ground track (Figure 4). Although originally conceptualized for snow and glacier studies, the ability to collect data over the same ground track will provide an assessment of the vegetation signal for potential change detection due to growth and disturbance.

PHOTON-COUNTING DETECTION, LASER WAVELENGTH, LASER SPOT SIZE

Science requirements to capture changes in land ice elevations and sea ice thickness led to the design of ATLAS aboard *ICESat-2*. ATLAS uses a photon-counting detection technology that enables a detection modality sensitive to individual photons, setting it apart from other laser ranging systems. A benefit of a photon-counting system is that the laser can operate at a relatively low power with a high pulse repetition rate, thus creating a near-continuous profile of measurements enabling distinction between ground and vegetation surfaces. A limitation, however, is that only a handful of photons are detected from each outgoing laser shot over vegetation, thus undersampling the vertical structure of vegetation. Unique from other space-based laser altimeters, the ATLAS instrument uses a green laser to actively map the surface elevation. The ATLAS instrument collects reflected light through a 0.8-m telescope via a narrow bandpass (30-p.m.) filter to the detector [2]. The laser repetition rate combined with the altitude and velocity of the satellite results in a 70-cm separation for each shot on Earth's surface in the along-track direction. Analyzing *ICESat-2* data over a geolocation validation corner cube array established at White Sands Missile Range, Magruder et al. [4] estimated each *ICESat-2* footprint to vary between 10 and 12 m in diameter. Although the geolocation of the photons within a footprint diameter is reported to be better than 5 m, true spatial uncertainty is closer to the footprint diameter since each photon can originate from any point within that area.

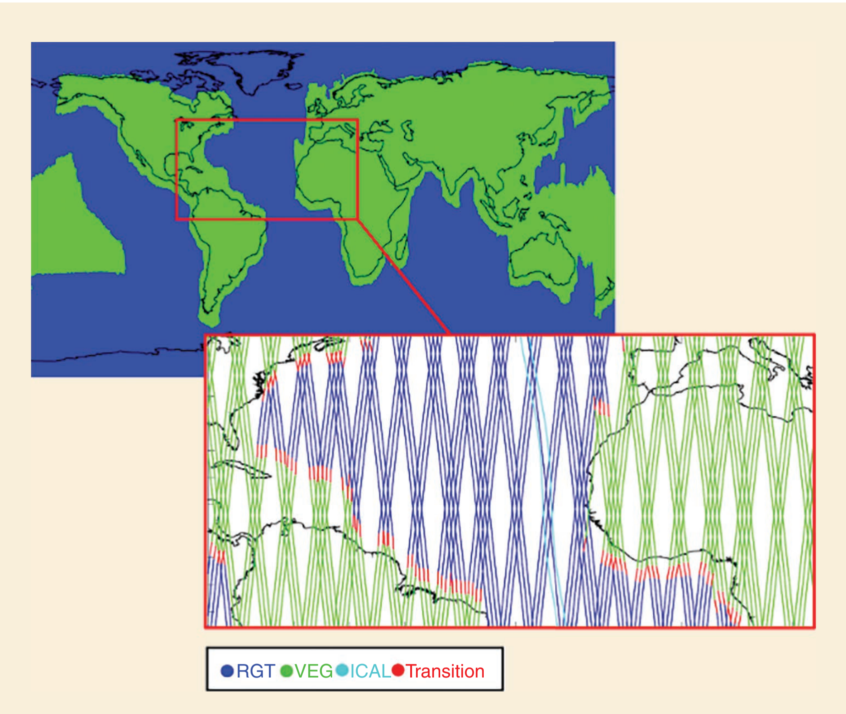

FIGURE 3. *ICESat-2* off-nadir pointing scheme, illustrating the RGT, VEG, and ICAL activities, and transition tracks. RGT: reference ground track; VEG: vegetation tracks; ICAL: instrument calibration. (Figure courtesy of Scott Luthcke, ICESat-2 Project Science Office.)

ATLAS uses a diffractive optical element to split the laser into six beams arranged as three pairs of beams approximately 3.3 km apart from one another [Figure 1(a) and (b)]. Each beam pair is approximately 3 km apart in the across-track direction and consists of strong and weak beams. The detection ratio between the strong and weak beam was designed to be approximately 4 to 1, and this detection ratio is observed over land ice [20]. Neuenschwander et al. [21], however, reported a detection ratio of approximately 2.5:1 over forested vegetation. Depending upon the surface reflectance and atmospheric conditions, up to 16 photons per outgoing shot could be detected on the 4 × 4 detector array for the strong beam and four photons on the weak beam detector. During the commissioning phase, the laser energy was set such that approximately nine photons per outgoing laser shot were detected over land ice [20] and zero to two photons per shot on average were detected over forested areas [21] because of the lower surface reflectance of forests. After four years in orbit, the laser energy had decreased by roughly 10%, leading the Project Science Office to increase the laser energy back to early mission levels. The key instrument and orbit parameters of *ICESat-2* are summarized in Table 1.

ATL08 LAND AND VEGETATION DATA PRODUCT

The algorithm developed to extract both terrain and canopy heights from the geolocated photon cloud (ATL03) utilizes a series of noise filters and surface fitting to estimate the ground surface and upper canopy surface (Figure 5) [3]. Based on the distribution of signal photons about the upper canopy and ground surface estimates, the ATL08 labels the individual photons as either noise, ground, canopy, or top of canopy photons [Figure 5(c) and (d)]. Next, statistics for both terrain and canopy detections are reported at a fixed 100-m segment size, based on the label at the photon level [Figure 5(e)]. The reported canopy statistics on ATL08 not only include the height of the canopy but also several canopy metrics (absolute and relative canopy statistics) that reveal information about the vertical distribution of the canopy photons and the structure of the vegetation. The ATL08 data product also provides indices for each labeled photon (i.e., ground, canopy, and top of canopy) to directly link to the ATL03 data product. These indices allow the user to calculate terrain and canopy height estimates at scales other than the 100-m segment size [22]. Each release of the *ICESat-2* data provides updates to the ranging calibrations of the raw photons as well as improvements to many of the higher level products. A unique capability of *ICESat-2* data is the near-continuous profile of both terrain and canopy heights. As observed in Figure 5, extracting heights even in

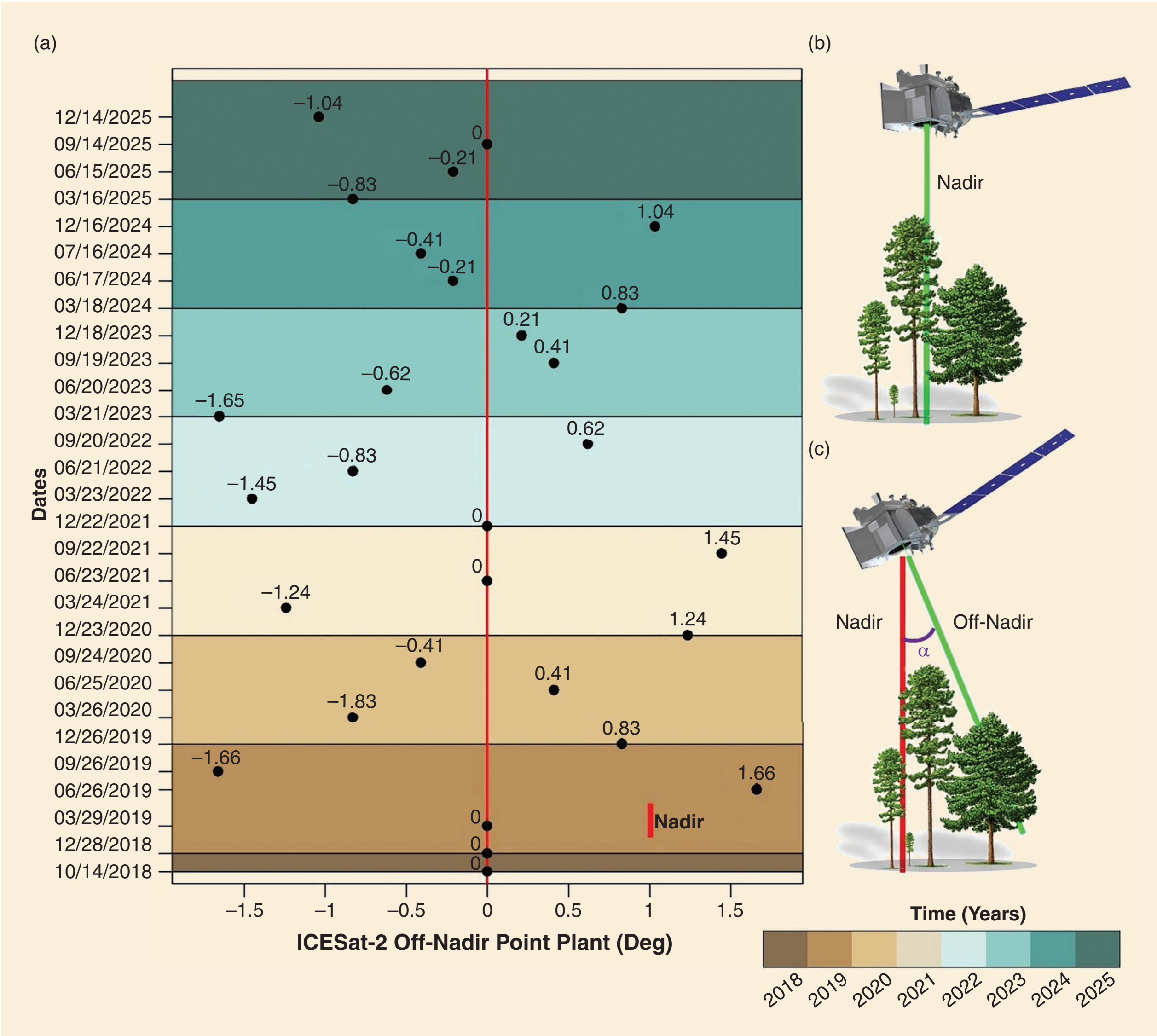

FIGURE 4. (a) *ICESat-2* off nadir pointing during the first seven years of operation. Illustration of *ICESat-2* operating at (b) nadir and (c) off-nadir. The vertical red line in (a) represents the nadir.

steep topography is a unique capability that is not feasible with large footprint systems. Among all of the *ICESat-2* products, ATL08 stands out as the most downloaded product (26,711,729 downloads by 31 December 2024) [Figure 6(a)]. The top five countries with the highest downloads of ATL08 data are (in descending order) China, the United States, India, Germany, and Canada [Figure 6(b)].

ATL18 PRODUCT (GRIDDED TERRAIN AND CANOPY HEIGHT)

The ATL18 product is currently under development, and an official release date has not yet been announced; however, the ATL18 Algorithm Theoretical Basis Document for Release 001 is dated 15 October 2025. The gridded product, ATL18, consists of gridded heights for both terrain and canopy and is derived from the height measurements reported on the ATL08 data product. The ATL18 gridded product provides global estimates of terrain and canopy heights at a nominal 1-km resolution; however, this spatial resolution might increase as more data are acquired over time. The ATL18 data product uses the Equal-Area Scalable Earth (EASE) 2.0 gridding scheme, which has also been adopted by the GEDI and Soil Moisture Active Passive [23] missions. EASE 2.0 is defined with respect to the World Geodetic System-84 ellipsoid (as is *ICESat-2*) and is compatible with the GeoTIFF file format. EASE 2.0 consists of a nested grid size (1, 3, and 9 km) and utilizes a Lambert polar projection. ATL18 serves as the only terrain product for all latitudes, including many of the Arctic islands that are not captured in the land ice data products. In the midlatitudes, EASE 2.0 adopts a cylindrical equal area global projection.

THE DEVELOPMENT OF SCIENTIFIC SOFTWARE TOOLS TAILORED TO WORK WITH *ICESAT-2* DATA HAS GREATLY ENHANCED ITS USE IN VEGETATION SCIENCE.

TABLE 1. ICESAT-2/ATLAS INSTRUMENT AND MISSION PARAMETERS.

PARAMETER	DESCRIPTION/VALUE
Laser type	Photon counting, 532 nm (green)
Pulse rate	10 kHz
Footprint diameter	10–12 m
Along-track spacing	70 cm
Beam configuration	Three pairs (six beams), ~3.3 km apart
Orbit altitude and inclination	454 km and 92°
Coverage	88° S to 88° N
Geolocation accuracy	~3 m (Release 006)
Repeat cycle	91 days
Data availability	Initial release in October 2018

For the initial version of the ATL18 data product, the layers for the gridded terrain products are calculated as the minimum, median, standard deviation, and range of surface and canopy height (h_te_best_fit_20m) from ATL08 within each 1-km grid cell. Future versions of ATL18 will explore additional gridding methods (e.g., inverse distance weighted from cell center). It is expected that the presence of snow on the surface will bias the estimated heights for certain locations. The first version of ATL18 terrain heights includes data from all seasons and conditions; however, the ATL18 development team collected data only in no-snow conditions with the understanding that, for certain latitudes, no-snow data may not exist. Terrain heights are calculated using all beams over all land cover types.

The ATL18 data product also consists of gridded canopy height estimates. Based on results from the literature showing the highest accuracy with the strong beam [24], [25], the gridded canopy heights are also derived from the strong beam data. Because the nominal resolution for the global gridded product is 1 km, ATL18 produces canopy height estimates stratified by land cover. The motivation for this stratification is to obtain better estimates of forested canopy heights that are often critical for conducting global carbon assessments. A 1-km pixel is often a composite of many land cover classes; thus, combining canopy heights of bare ground/grasslands/shrubs with forest canopy heights would result in a lower estimation of forest canopy height than that obtained by only considering the heights of forested segments. The ATL18 canopy product consists of statistics derived from the top canopy height computed at 20-m segments (ATL08-derived h_canopy_20m attribute) in each 1-km grid cell, calculated separately for forest classes and all land cover classes. Figure 7 provides an illustration of the ATL18 product. In this example, the global canopy height map at 1-km resolution was derived from the median canopy height of all strong beam ATL08 segments (Release 005) within each grid cell for the first four years of data collection (2019 through 2022). Of the possible 135 million 1-km grid cells over land, only 56% are occupied by at least one ATL08 segment (Figure 7). Beyond the canopy heights shown in Figure 7, ATL18 includes additional filtering protocols to remove the impact of low-lying clouds on the estimation of canopy heights (see Greenland).

TOOLS

ICESat-2 has been a groundbreaking mission for a wide range of scientific research applications [14], and the development of scientific software tools tailored to work with *ICESat-2* data has greatly enhanced its use in vegetation science. It has become pivotal for scientists to share resources to enhance the transparency and reproducibility of scientific results. Thus, it is critical to highlight existing tools to enhance open science. These data tools facilitate efficient data access, reading, visualization, and format conversion.

Reading and format conversion are particularly critical since *ICESat-2* data are distributed in a Hierarchical Data Format (HDF5) [26], a hierarchical file system-like data structure format, which can be challenging to work with directly. Tools that simplify the reading and conversion of *ICESat-2* data to prominent and commonly used formats, such as ASCII text files, are critical to making the data more accessible and interpretable for researchers. The data visualization capability is also crucial for exploration, interpreting *ICESat-2* data across various environments, understanding the impacts of various physical phenomena and atmospheric interactions, and for general communication. For example, visualizing *ICESat-2* data acquired during the day or night can inform the effect of solar background illumination on data quality and the influence of canopy cover on photon penetration in different ecosystems and can also provide insights into algorithmic choices for noise filtering and photon classification [27].

Available *ICESat-2* data tools come in various types, including stand-alone software, e.g., PhotonLabeler [27] and Photon Research and Engineering Analysis Library (PhoREAL) [28], web-based cloud applications (e.g., SlideRule [29], OpenAltimetry [30], and ICEComb [31]), and programming packages (e.g., icepyx [32], PhoREAL [28], earthaccess [33], IceSat2R [34], and ICESat2VegR [35]). These *ICESat-2* data tools cater to the various needs and expertise of researchers (Table 2). Standalone GUI applications provide an intuitive interface for

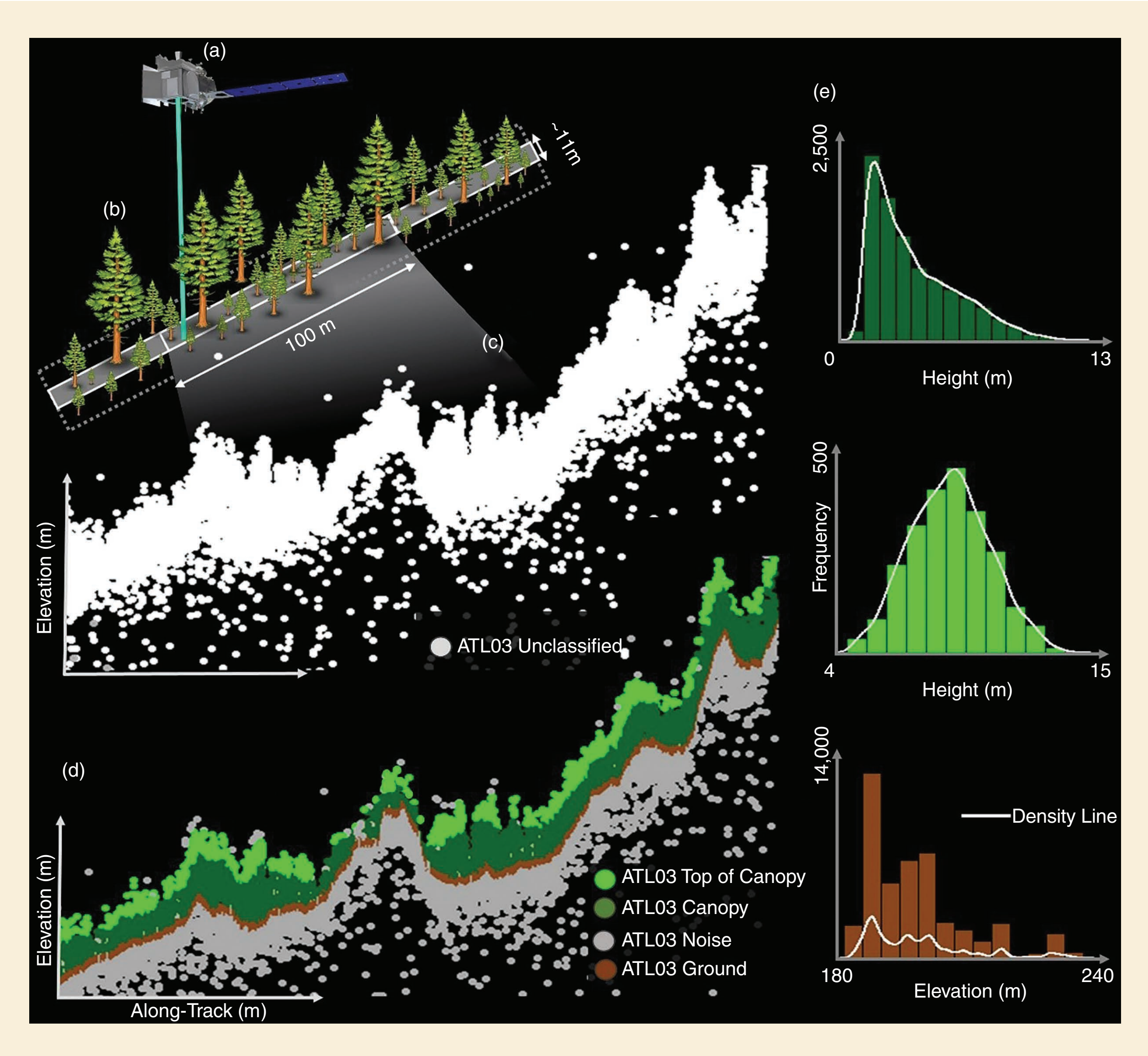

FIGURE 5. How the ATL08 terrain and canopy height are computed at 100-m segment size from labeled ATL03 photons. (a) *ICESat-2* laser beam over a (b) Canadian boreal forest transect. (c) Unclassified ATL03 photons (ATL03_20181210060430_11090106_961a4_01_gt1r) and (d) ATL03 labeled photons from ATL03 and ATL08 products, illustrating that determination of terrain elevation and vegetation heights is feasible even in areas with significant topographic relief. (e) The computed distribution of ATL08 terrain and canopy attributes.

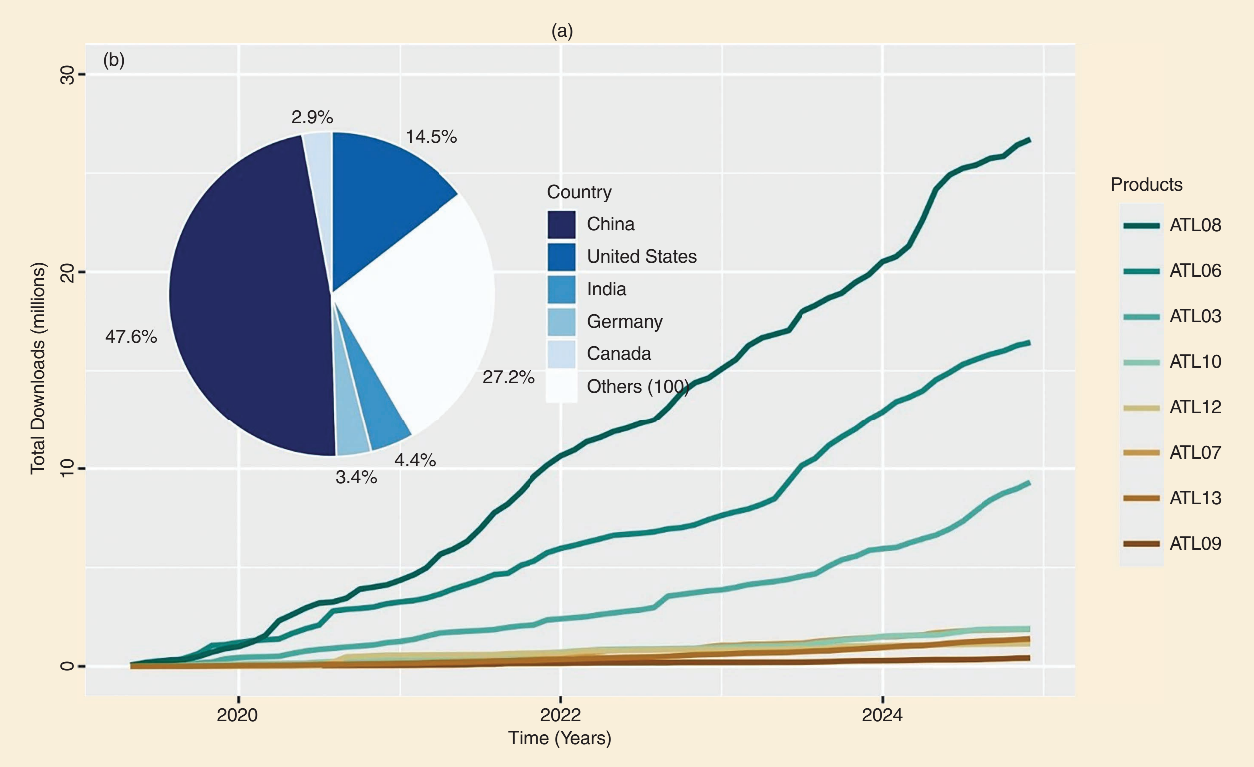

FIGURE 6. (a) Number of total downloads of all *ICESat-2* products over time and (b) percentage of ATL08 downloads by countries (top five) by 31 December 2024. (Statistics provided by NSIDC DAAC.)

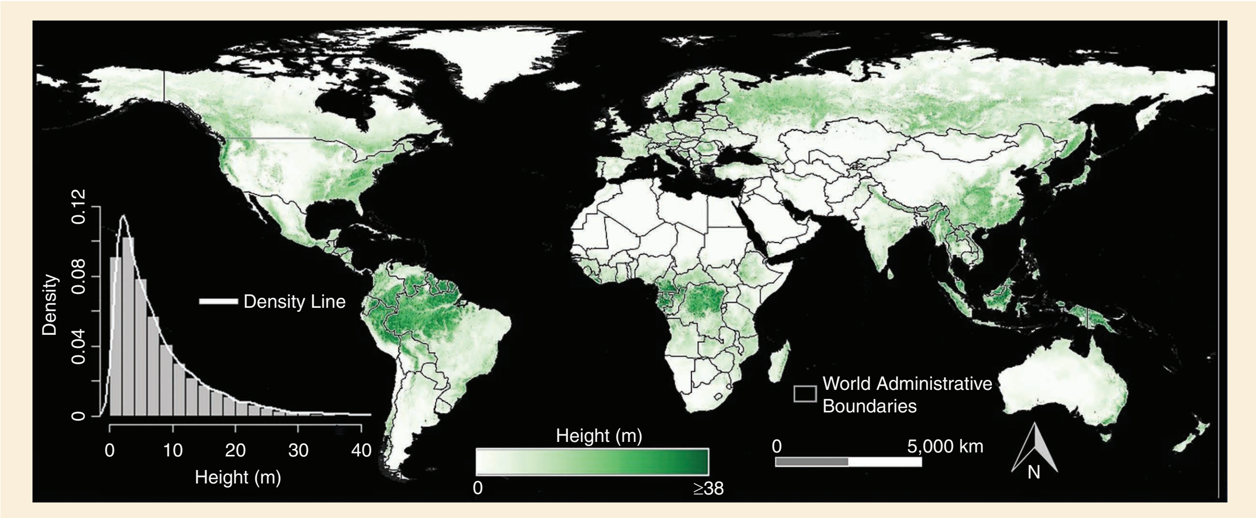

FIGURE 7. Illustration of the ATL18 canopy height product at 1-km spatial resolution at the global scale. The height values represent the median of all ATL18 height estimates within a given grid size of 1 km.

visualizing and manipulating *ICESat-2* data, making it more accessible to scientists who may not have advanced programming skills. For instance, the PhotonLabeler (Table 2) can be used to visualize and label individual photons, which can support validation studies [27]. Web-based tools offer wide accessibility while negating the need for expensive computing hardware, which expedites data exploration and analysis. Programming packages, such as ICESat2VegR [35], IceSat2R [34], and icepyx [32], enable researchers with coding proficiency to develop customized solutions and automate complex data processing tasks, allowing for greater flexibility in addressing vegetation-related research questions. Table 2 outlines data tools, though it is not an exhaustive list of all tools that have been developed by scientists in the vegetation community.

TABLE 2. SUMMARY OF *ICESAT-2* DATA TOOLS FOR LAND AND VEGETATION APPLICATIONS.

NAME AND CITATION	TYPE	DESCRIPTION, PURPOSES, AND AVAILABILITY
ICESat2VegR [36]	Programming package (R)	An R Package for ICESat-2 Data Processing and Visualization for Land and Vegetation Applications. The package is available in GitHub at https://github.com/carlos-alberto-silva/ICESat2VegR
IceSat2R [34]	Programming package (R)	An R package for ICESat-2 Altimeter Data using R. The package is available at CRAN: https://cran.r-project.org/web/packages/IceSat2R/index.html
PhotonLabeler [27]	Stand-alone tool	Free compiled MATLAB GUI, reading, visualization and manual labeling of *ICESat-2* Geolocated Photon data (ATL03). The software is available from https://github.com/Oht0nger/PhoLabeler
PhoREAL [28]	Stand-alone tool	PhoREAL is a geospatial analysis toolbox that allows users to read, process, analyze, and resample ATL03 and ATL08 data into user-specified along-track distances in the form of figures and popular file formats, such as lidar LAS, comma-separated values text files, and Keyhole Markup Language. Download from https://github.com/icesat-2UT/PhoREAL
SlideRule [29]	Stand-alone tool (web based)	A public web service with representational state transfer application programming interfaces for processing science data and returning results. A cloud-native framework that supports access and visualization of *ICESat-2* data in the cloud. More details on signing up and using the platform may be accessed here: https://slideruleearth.io/web/.
icepyx [32]	Programming package (Python)	A Python-based software library for obtaining and working with *ICESat-2* data locally and in the cloud; improves interoperability for *ICESat-2* datasets with other open source tools. icepyx is available on GitHub (https://github.com/icesat2py/icepyx)
earthaccess [33]	Programming package (Python)	A Python library to search, download, or stream NASA Earth science data including *ICESat-2* data: https://github.com/nsidc/earthaccess
xATLy [37]	Programming package (MATLAB)	A MATLAB toolbox that facilitates reading, visualization, and processing of ATL03 and ATL08 in HDF5 format with the end goal of generating customized along-track terrain and canopy height datasets: https://github.com/Oht0nger/xATLy
OpenAltimetry [30]	Stand-alone tool (web-based)	A web-based cyberinfrastructure platform that allows users to locate, visualize, and download *ICESat-2* surface elevation data and photon clouds for any location on Earth, on demand: https://doi.org/10.1007/s12145-020-00520-2
ICEComb [31]	Stand-alone tool (web-based)	The ICEComb tool offers a robust web-based visual environment, primarily serving as a platform for data processing, analysis, and visualization of laser altimeter data from the ICESat and ICESat-2 missions: https://doi.org/10.3390/software3030020

LITERATURE REVIEW ON ICESAT-2 FOR TERRESTRIAL APPLICATIONS

METHODS APPLIED IN THE LITERATURE REVIEW

The details of our systematic literature search are outlined in Table 3, encompassing the databases employed (Web of Science and Scopus), the specific keywords utilized, the defined search period, targeted document types, and language considerations. Herein, our focus was solely on English-language articles incorporating the keyword "ICESat-2" in titles, abstracts, or keywords, limited to "Article" or "Review" document types. The review considered articles published between 2014 and 2024, spanning from the first land and vegetation research following the release of the ICESat-2 simulator Multiple Altimeter Beam Experimental Lidar (MABEL) to the year we began the analysis (Table 3). The complete query string used for the Web of Science platform was "TS=(ICESat-2) AND LA=(English) AND DT=(Article OR Review) AND PY=(2014—2024)", and "(TITLE-ABS-KEY (icesat-2) AND LANGUAGE (english)) AND PUBYEAR > 2013 AND PUBYEAR < 2025 AND (LIMIT-TO (DOCTYPE, "ar") OR LIMIT-TO (DOCTYPE, "re"))" for Scopus. The final search date was 31 December 2024, with Web of Science and Scopus yielding record counts of 826 and 792, respectively. We applied the Preferred Reporting Items for Systematic Reviews and Meta-Analyses (PRISMA) flow diagram [38], [39] for the identification, screening, eligibility assessment, and inclusion of the articles. Record identification involved executing searches in Web of Science and Scopus, followed by the removal of duplicates, resulting in 849 unique records across both databases (Figure 8).

TABLE 3. SEARCH CONDITIONS FOR THE APPLICATION DATABASE.

SEARCH ATTRIBUTES	SEARCH PARAMETERS
Database	Web of Science and Scopus
Keyword	ICESat-2
Publication year	2014–2024
Document type	Research article or review
Language	English
Searching date	12/31/2024

In this review, as we are only interested in articles focused on land and vegetation applications, we categorized the articles within Earth system classifications, with those not aligning with these classes (e.g., articles about instrument calibrations) grouped separately as "Nonspecific" (Table 4). Subsequent record screening involved manual inspection of titles and abstracts, selecting articles within the biosphere (n = 199) and lithosphere (n = 128) classes and across nine

TABLE 4. SEARCH CONDITIONS FOR THE APPLICATION DATABASE.

EARTH SYSTEM	ARTICLES IDENTIFIED	ARTICLES INCLUDED IN THIS REVIEW
Atmosphere	11	0
Biosphere	199	178
Cryosphere	208	0
Hydrosphere	254	0
Lithosphere	128	104
Nonspecific	49	11
Total	849	293

TABLE 5. LAND AND VEGETATION APPLICATIONS.

APPLICATION	DESCRIPTION
Forestry	Studies focused on estimating vegetation height, cover, volume, basal area, and fuels
Ecology	Studies focused on modeling biomass, carbon, forest diversity, LAI, habitat quality, and wildlife
Disturbance	Studies focused on disturbance events, such as fire, tropical cyclones, and drought, and their impacts on vegetation
Education	Studies focused on education of the ICESat-2 mission focused on land and vegetation applications
Tools	Studies focused on the development of tools for *ICESat-2* data processing and analysis
Urban	Studies focused on the urban landscape, including the height of buildings and road attributes
Land use	Studies focused on land use
Methods	Studies focused on methods and algorithm development for land and vegetation applications
Terrain	Studies focused on terrain elevation estimation and modeling.

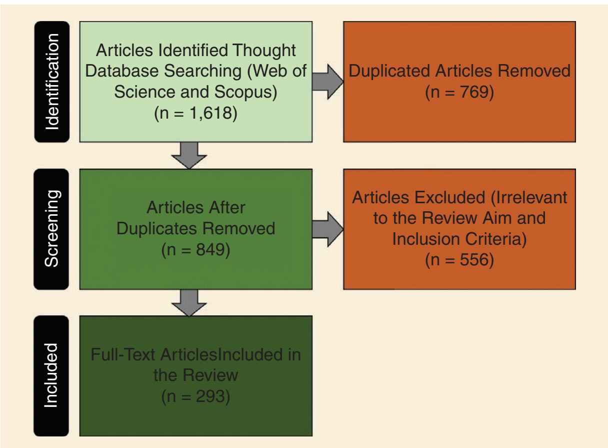

FIGURE 8. PRISMA flow diagram showing the systematic literature review protocol, along with the number of articles identified, excluded, and included in the review.

land and vegetation application categories (Table 5). After applying these inclusion criteria during the full-text assessment, 293 records were identified as meeting the criteria and were consequently included in the review analysis (Table 4). Conversely, 556 records were excluded for not focusing on land and vegetation applications (Figure 8). The 293 selected articles served as the foundation for a comprehensive table, incorporating key information such as the first author, DOI link, title, Earth system class, application class, study area location (country or territory, and continent), keywords, abstract, journal, and publication year. The complete list of the 293 articles can be found in the supplementary data file, available at https://doi.org/10.1109/MGRS.2026.3666794, provided by the authors.

RESULTS OF THE LITERATURE REVIEW

DISTRIBUTION OF ICESAT-2 PUBLISHED STUDIES BY GEOGRAPHY, BIOME, AND APPLICATION

The emergence and global interest in *ICESat-2* for land and vegetation applications was evident from the bibliographical analysis [Figure 9(b)], which showed that the majority of studies originated from Asia (38.3%), followed by North America (33.9%), and Europe (11.4%); see Figure 9(a). Nine articles were conducted at the global scale [40], [41], while other studies focused on smaller scales, mostly in the United States and China (n = 204) [Figure 9(a); the total number of studies by biome exceeds the total number of articles analyzed since a single study can encompass more than one biome]. Abdalati et al. [42] introduced the ICESat-2 mission, and McGill et al. [43] developed the MABEL ICESat-2 simulator, but the first articles describing the potential of *ICESat-2* specifically for land and vegetation applications emerged in 2014 [44], [45], [46], coinciding with the prelaunch preparation of the ICESat-2 mission. Interest remained modest for about four years, resulting in 21 articles (7.2%) by 2018 prelaunch of the mission. From 2019 to 2023, the number of studies (272 articles, 92.8%) focusing on land and vegetation applications increased exponentially, bringing the cumulative total to 293 articles by 2024 [Figure 9(b)]. The number of studies conducted in high-income economies (n = 118, see, e.g., Montesano et al. [8] and Silva et al. [10]), as classified by the World Bank [47], and middle-to-low-income economies (n = 156, see, e.g., Davenport et al. [48] and Stovall et al. [49]) were approximately similar, with some studies conducted in both (n = 19, see, e.g., Liu et al. [50] and Yu et al. [51]).

Studies encompassed multiple terrestrial biomes; see Table 6, Figure 10(a), and [52]. The majority of studies focused on temperate and tropical regions with three terrestrial biomes comprising more than 50% of all studies: TeBrMix (n = 130; 28.8%; e.g., Jiang et al. [53], Popescu et al. [54], and Xi et al. [55]), TrBrMoist (n = 64; 14.2%; e.g., Fernandez-Diaz et al. [56] and Zang et al. [57]), and TeCo (n = 63; 14%; e.g., Liu and Popescu [58] and Narine et al. [59], [60]). By contrast, Tundra (n = 3; 0.7%) and tropical

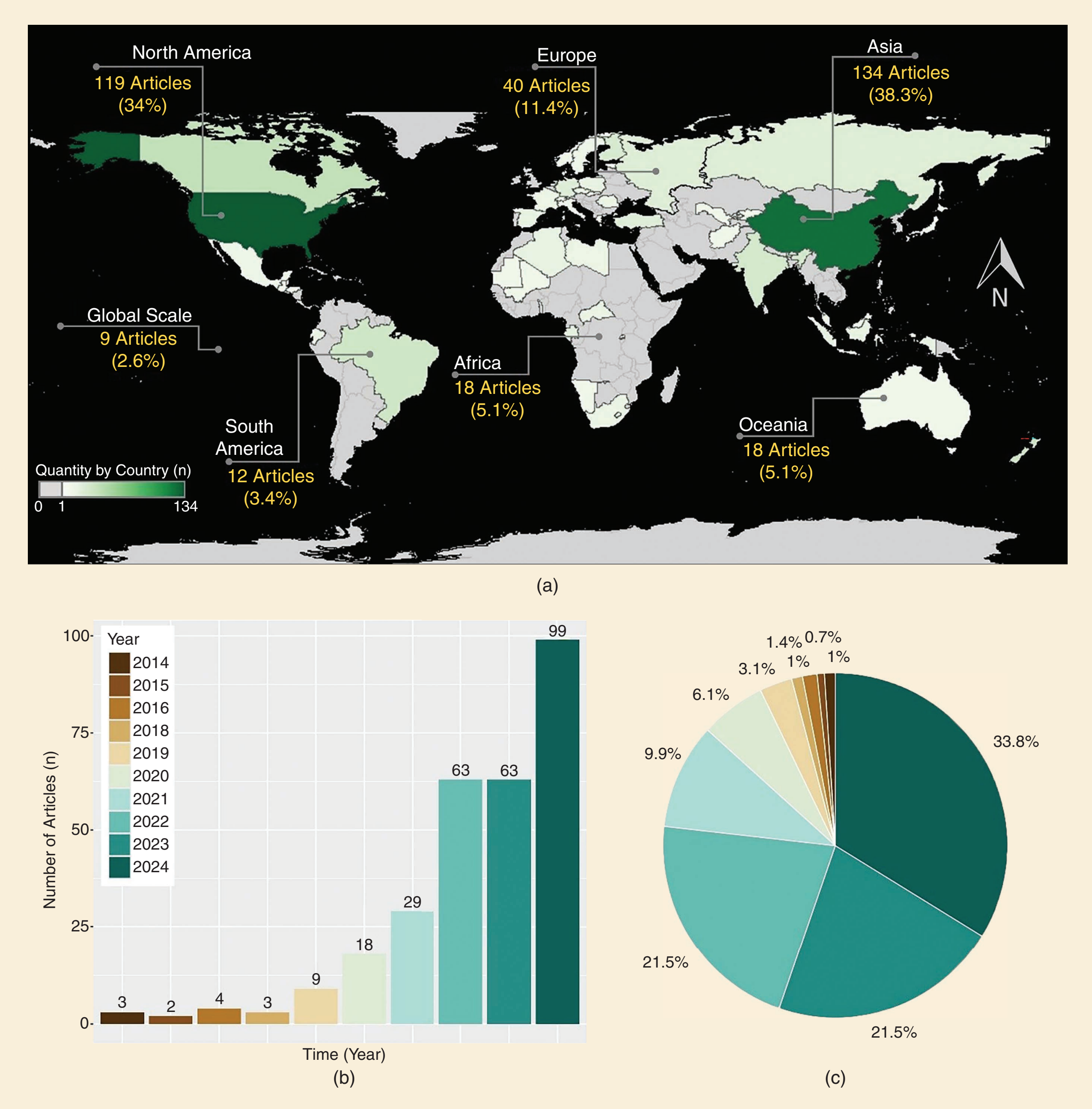

FIGURE 9. (a) Geographical distribution of the study sites by country (provided by the green color bar) and continents (highlighted in the text). Fifty-nine articles' study sites were carried out in more than one country. (b) Frequency distribution and (c) percentage of articles published since 2014.

coniferous forests (TrCo; n = 2; 0.5%) are the least represented [Figure 10(a) and (b); [61]).

Considering the application categories [Figure 10(b) and (c)], we observed that the majority of studies were focused on "Forestry" (n = 95; 32.4%, e.g., Narine et al. [59], Wu and Shi [62], and Xi et al. [55]), "Terrain" (n = 69; 23.5%, e.g., Tian and Shan [63], Zhu et al. [64], and Wu et al. [65]), "Methods" (n = 50; 17.1%, e.g., Huang et al. [66] and Zhang and Kerekes [44]), and "Ecology"' (n = 38; 13%, e.g., Guo et al. [67], Purslow et al. [68], and Zhang et al. [69]) applications. By contrast, "Tools"' were less predominant, with only two studies [27], [31]. Despite the increased number of studies focused on "Disturbance" and "Land Use" applications from 2020 to 2024, "Forestry," "Terrain," "Ecology," and "Methods" have consistently remained the most frequent areas of application.

The studies found were published in several journals across various disciplines, with *Remote Sensing* being the most prominent [Figure 10(e)]. Over the years, we observed that *Remote Sensing* (n = 65; 22.2%; e.g., Malambo and Popescu [27], Narine et al. [9], and Neuenschwander and Magruder [70]), *Remote Sensing of Environment* (n = 30;

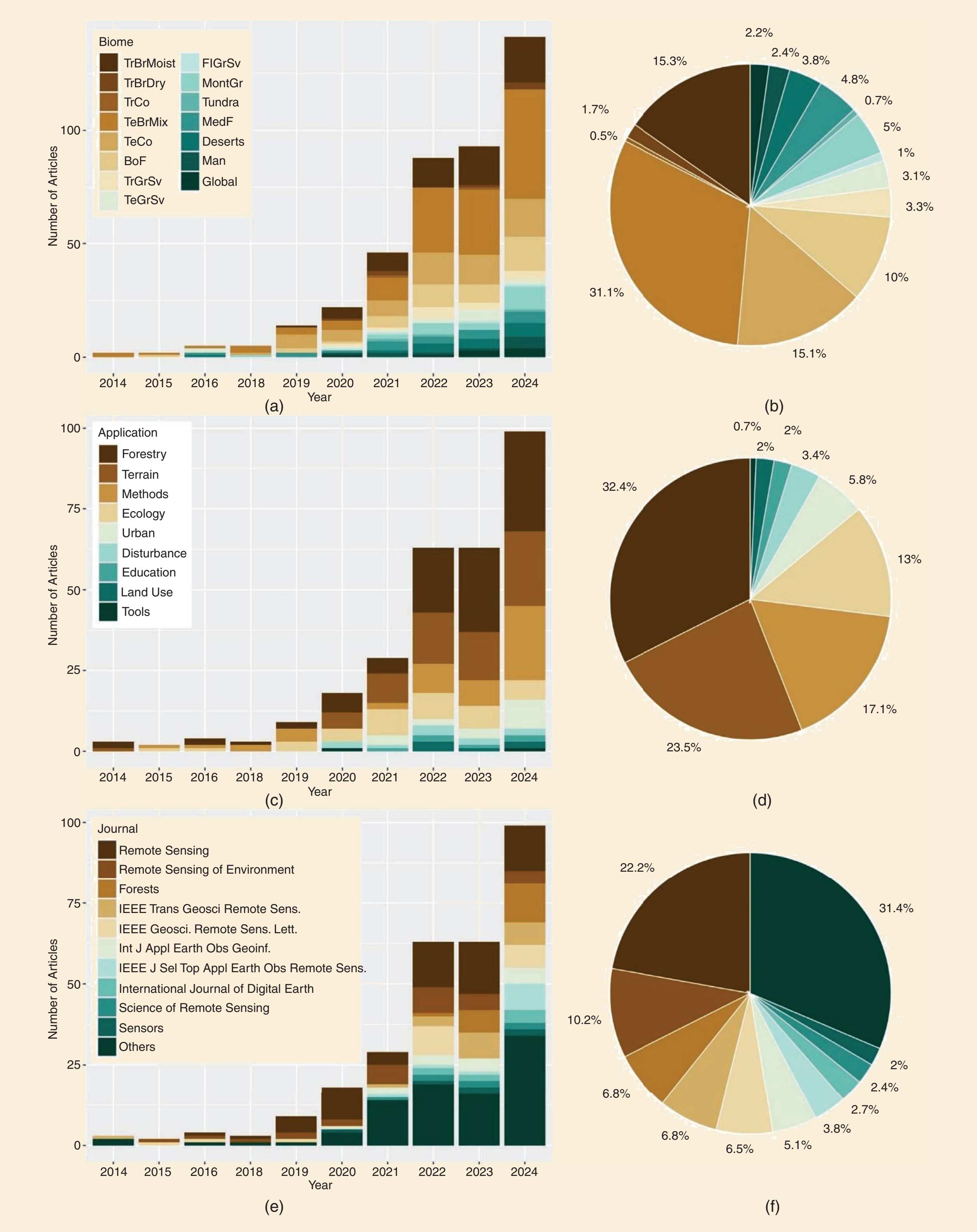

FIGURE 10. Frequency distribution and percentage of ICESat-2 articles across (a), (b) terrestrial biomes, (c), (d) applications, and (e), (f) journal types. TrBrMoist: Tropical and Subtropical Moist Broadleaf Forests; TrBrDry: Tropical and Subtropical Dry Broadleaf Forests; TrCo: Tropical and Subtropical Coniferous Forests; TeBrMix: Temperate Broadleaf and Mixed Forests; TeCo: Temperate Coniferous Forests; BoF: Boreal Forests/Taiga; TrGrSv: Tropical and Subtropical Grasslands, Savannas, and Shrublands; TeGrSv: Temperate Grasslands, Savannas, and Shrublands; FlGrSv: Flooded Grasslands and Savannas; MontGr: Montane Grasslands and Shrublands; Tundra: Tundra; MedF: Mediterranean Forests, Woodlands, and Scrub; Deserts: Deserts and Xeric Shrublands; Man: Mangroves; Global: Global.

10.2%; e.g., Duncanson et al. [7], Neuenschwander and Pitts [3], and Silva et al. [10]), *Forests* (n = 20, 6.8%; e.g., Cheng et al. [71], Doyog and Lin [72], Song et al. [73]), and *IEEE Transactions on Geoscience and Remote Sensing* (n = 19, 6.5%; e.g., Pan et al. [74], Yang et al. [75], and Yu et al. [76]) are the top four journals from a list of 77 journals [Figure 10(e) and (f)].

DISTRIBUTION OF *ICESAT-2* DATA PRODUCTS AND METHODS IN PUBLISHED STUDIES

ICESat-2 photon-counting lidar is processed into five levels of data products. Within Level 2 data products is ATL03, which provides geolocated photon data. The Level 3 ATL08 photon product provides four levels of classified photons: noise (0), ground level (1), canopy/vegetation level (2), and top of canopy (3). Across 293 studies using *ICESat-2* data, 15.7% used ATL03 only, and 29.4% combined ATL03 with ATL08 [Figure 11(a)]. Most ATL03-based studies were located in TeBrMix (24%), TrBrMoist (13.3%), and TeCo (12%). Additionally, 23.9% of the studies fused *ICESat-2* data with other sources, 60.9% produced models, and 32.6% used artificial intelligence approaches.

Common uses of ATL03 include photon classification (30.4%), terrain elevation (28.3%), height estimates (32.6%), and other uses (8.7%) (Table 7). Photon classification studies primarily focused on developing methods for canopy–ground classification and noise filtering. Reported performance metrics showed F1-scores ranging from 0.84 to 0.99, recall from 0.84 to 1, and precision from 0.87 to 1. For instance, Yang et al. [77] achieved an F1-score, recall, and precision of 0.99 using an elliptical distance-based method in MedF and TeBrMix. By contrast, Wang et al. [78] applied an improved Density-Based Spatial Clustering of Applications with Noise (DBSCAN)-based denoising algorithm specifically in Mediterranean forests, achieving a performance with an F1-score of 0.86, a recall of 0.84, and a precision of 0.87. Terrain elevation studies aimed to generate, refine, or validate digital elevation models (DEMs). Among those reporting results, the coefficient of determination (R^2) ranged from 0.74 to 1, and the root-mean-square error (RMSE) ranged from 0.03 to 6.7 m. In TeBrMix, Zhang et al. [79] improved stereoscopic positioning through a joint block adjustment, achieving an R^2 value of 0.99 and an RMSE of 0.50 m. Zhu et al. [80] estimated terrain slopes from ATL03 data using along/across-track and plane-fitting methods in TeBrMix, achieving an R^2 of 0.87 and a ground elevation RMSE of 2.47 m. Studies targeting height estimates of both canopy and buildings reported R^2 values between 0.54 and 0.98 and RMSE values ranging from 0.35 to 8.1 m, reflecting varying levels of accuracy depending on the environment. Lao et al. [81] retrieved building heights in Haidian, Beijing, China, with an R^2 of 1 and an RMSE of 0.35 m. By contrast, Huang et al. [82] mapped forest height in mountainous terrain with an R^2 of 0.87 and an RMSE of 3.18 m. A few studies extended the use of ATL03 to other applications, such as estimating forest biomass, LAI, and land use. For instance, Narine et al. [9] estimated aboveground biomass in temperate coniferous forests, achieving an R^2 of 0.58 and an RMSE of 23.89 Mg/ha. Similarly, Guo et al. [67] retrieved a LAI in TeGrSv with an R^2 of 0.5 and an RMSE of 0.37.

A total of 132 studies (45.1%) analyzed used only ATL08, while 86 (29.4%) combined it with ATL03. ATL08 data are officially available at a 100-m segment size, but 19 studies adjusted this scale to meet their objectives, while

TABLE 6. THE TERRESTRIAL BIOME CLASSIFICATION AND THEIR SPECIFIC ABBREVIATIONS CONSIDERED IN THIS STUDY.

TERRESTRIAL BIOMES	ABBREVIATION
Tropical and Subtropical Moist Broadleaf Forests	TrBrMoist
Tropical and Subtropical Dry Broadleaf Forests	TrBrDry
Tropical and Subtropical Coniferous Forests	TrCo
Temperate Broadleaf and Mixed Forests	TeBrMix
Temperate Coniferous Forests	TeCo
Boreal Forests/Taiga	BoF
Tropical and Subtropical Grasslands, Savannas, and Shrublands	TrGrSv
Temperate Grasslands, Savannas, and Shrublands	TeGrSv
Flooded Grasslands and Savannas	FlGrSv
Montane Grasslands and Shrublands	MontGr
Tundra	Tundra
Mediterranean Forests, Woodlands, and Scrub	MedF
Deserts and Xeric Shrublands	Deserts
Mangroves	Man
Global	Global

TABLE 7. EXAMPLES OF STUDIES FROM THE LITERATURE REVIEW ASSESSING THE PERFORMANCE OF *ICESAT-2* ATL03.

AUTHOR	BIOME	TARGET	PERFORMANCE ASSESSMENT
[77]	TeBrMix and MedF	Photon classification	F1-score: 0.99 Recall: 0.99 Precision: 0.99
[78]	MedF	Photon classification	F1-score: 0.86 Recall: 0.84 Precision: 0.87
[79]	TeBrMix	Terrain elevation	R^2: 0.99 RMSE: 0.50 m
[84]	TeBrMix	Terrain elevation	R^2: 1 RMSE: 0.69 m
[81]	Not applicable	Height estimates (building)	R^2: 1 RMSE: 0.35 m
[82]	TeCo	Height estimates (canopy)	R^2: 0.87 RMSE: 3.18 m
[9]	TeCo	Biomass	R^2: 0.58 RMSE: 23.89 Mg/ha
[67]	TeGrSv	LAI	R^2: 0.5 RMSE: 0.37

R^2: coefficient of determination; RMSE: root-mean-square error.

six studies tested different segment sizes along with the standard 100 m. Nine studies employed a 20-m segment size, one study employed 30-m segments, and another used 90-m segments.

Here we found articles that used ATL08 data and were applicable to terrain elevation and building height topics (n = 54; 24.8%). From all articles that used ATL08 data to address topics related to terrain elevation, the most explored biomes were TeBrMix (31.6%), TrBrMoist (16.3%), and TeCo (13.3%). In addition, two articles validated DEMs using ATL08 data at the global scale [85], [86]. From the included 61 articles, 19 reported using machine learning within the analysis, 35 produced or incorporated models, and 16 fused *ICESat-2* data with other sources. Among articles that only used ATL08 data to quantify terrain elevation, the reported R^2 values ranged from 0.65 to 1, with the RMSE ranging from 0.12 to 10.2 m. Within these applications, multiple objectives were investigated. Narin and Gullu [87] performed vertical accuracy assessments for multiple global DEMs and ATL08 in different locations using airborne laser scanning (ALS) as ground truth. R^2 across all datasets and locations ranged from 0.89 to 1, while the RMSE ranged from 7.85 to 13.75 m for ATL08 and from 6.17 to 22.35 m for other DEM products. Hu et al. [88], on the other hand, proposed a method to enhance the accuracy of an interferometric SAR-derived DEM under forest canopy interference using ATL08 as control points; R^2 values ranged from 0.71 to 1 and RMSE values from 2.78 to 28.09 m. Other applications and their performances can be found in Table 8.

From 293 articles, 114 (38.9%) were related to canopy height, cover, LAI, and biomass. A total of 77 out of 114 (67.5%) articles used ATL08 products, while 37 (32.5%) combined ATL08 with ATL03. Canopy height estimation derived from ATL08 data demonstrated an average relative RMSE of 26.6% with a standard deviation of ±14.6%. Other averages returned an R^2 of 0.68, an RMSE of 3.76 m, and a relative bias of 12.1%. These accuracy metrics varied across biomes, with better performance observed in TeBrMix (average RMSE = 14.7%) compared to other biomes (average RMSE = 27.3%). At the global scale, Ma et al. [89] assessed global vegetation vertical structure using the ecosystem demography model calibrated with *ICESat-2* observations, while Yu et al. [90] mapped global mangrove canopy height by integrating multisource remote sensing data, achieving an R^2 of 0.88 and an RMSE of 29.9%. Although canopy height assessments using ATL08 were conducted across 14 biomes [Figure 11(f)], most canopy-related studies were concentrated in TeBrMix (30.3%), TrBrMoist (14.4%), BoF (13.6%), and TeCo (12.1%), accounting for 70.4% of the scrutinized studies. This uneven distribution of studies across biomes highlights the importance of considering sample size when interpreting these findings despite the potential for canopy height estimation to be applied across multiple biomes [Figure 11(f)]. For instance, Zhang and Liu [91] reported an RMSE between 4.49 m and 6.33 m (R^2 = 0.13–0.44) in BoF forests (Table 8), while Rodda et al. [92] observed similar results in a TrBrMoist (RMSE from 3.50 to 12.5 m, and R^2 from 0.05 to 0.46). For canopy height estimation, bias values were low, with means ranging from 0.72 ± 0.76 m. Some studies have indicated underestimation of height retrievals. Similarly, Mulverhill et al. [93] reported a bias

TABLE 8. EXAMPLES OF STUDIES FROM THE LITERATURE REVIEW ASSESSING THE PERFORMANCE OF ICESAT-2'S ATL08.

AUTHOR	BIOME	TARGET	SEGMENT SIZE (M)	REFERENCE DATASET	PERFORMANCE
[102]	MontGr	Terrain elevation	100	ALS	R^2: 0.98 RMSE: 0.14 m
[103]	Not applicable	Height estimates	100	ALS	R^2: 0.99 RMSE: 0.41 m
[91]	BoF	Canopy height	100	ALS	R^2: 0.44 RMSE: 4.49 m
[92]	TrBrDry	Canopy height	100	ALS	R^2: 0.46 RMSE: 3.5 m
[104]	TeBrMix	Canopy cover	100	ALS	R^2: 0.86 RMSE: 0.21
[105]	TeBrMix	Canopy cover	100	Field measurements	R^2: 0.75 RMSE: 0.09
[73]	TrBrMoist	Aboveground biomass	100	N/A	R^2: 0.43 RMSE: 5.29 Mg/ha
[106]	TeCo	Aboveground biomass	100	ALS	R^2: 0.79 RMSE: 19.16 Mg/ha
[100]	TrBrMoist	LAI	20, 100, and 200	ALS	R^2: 0.63 RMSE: 2.33 m^2/m^2
[71]	TrBrMoist	Forest age	100	Field measurements	R^2: 0.67 RMSE: 12.8 years
[101]	TrBrMoist	Species diversity	100	NA	R^2: 0.64 RMSE: 0.27

of 0.55 m (4.2%), emphasizing a relatively low systematic error in height estimation.

Canopy cover estimation derived from ATL08 data revealed RMSE values ranging from 11.0% to 14.7% and R^2 from 0.75 to 0.86. Contrasting canopy cover accuracies from ATL08 were observed between TeBrMix (RMSE = 11.0%) and TeCo (RMSE = 14.7%). Unlike canopy height studies, canopy cover assessments derived from ATL08 data were conducted in only five biomes: TrBrMoist, TrCo, TeBrMix, TeCo, and MedF [Figure 11(f)], with studies well

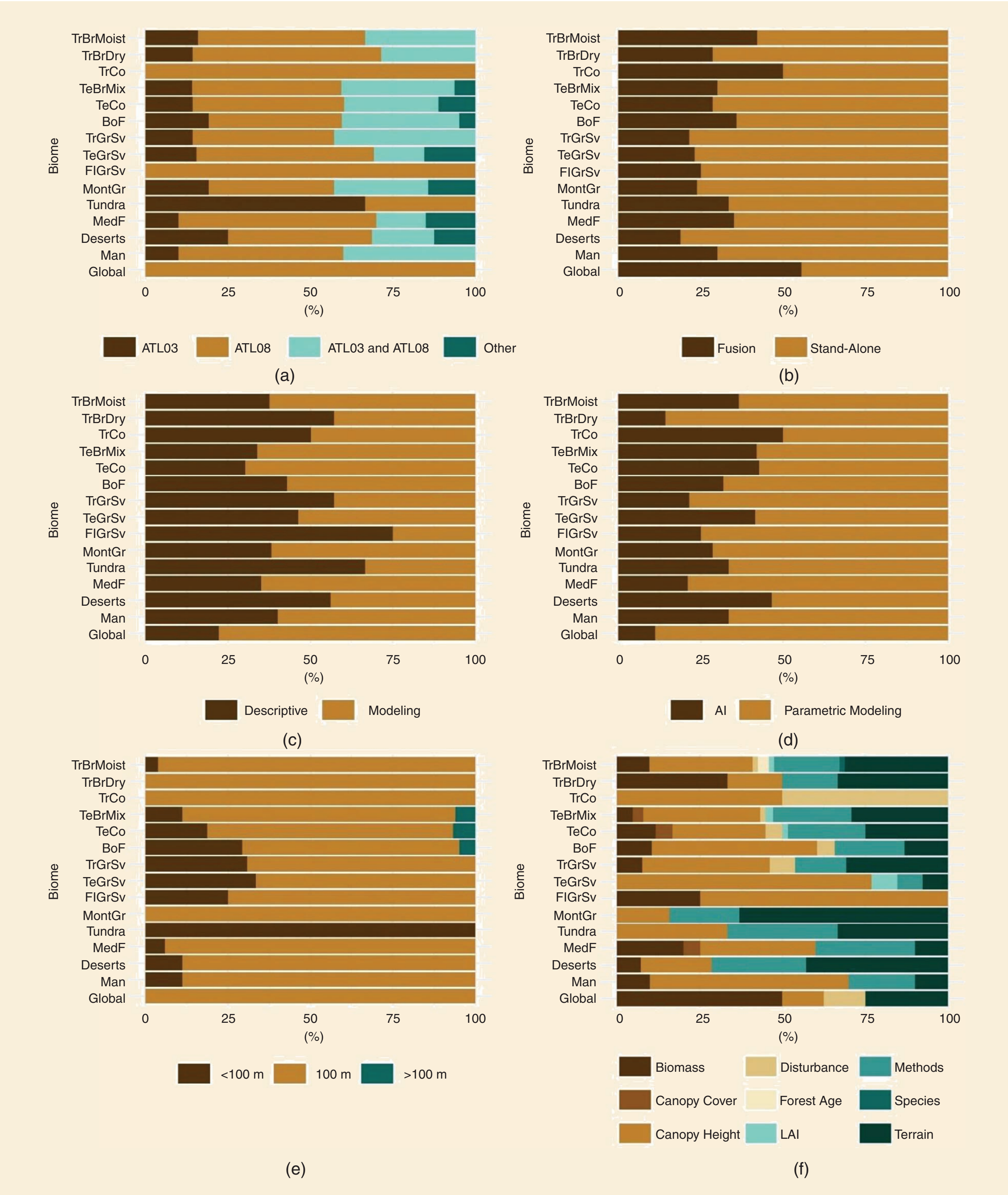

FIGURE 11. Percentage distribution of key factors in ICESat-2 literature across terrestrial biomes. Key factors include (a) ATL source, (b) ATL fusion (stand-alone or fused), (c) ATL implementation methods, (d) algorithm type, (e) ATL08 segment size type, and (f) ATL application. AI: artificial intelligence.

distributed across biomes. Notably, further research should be conducted in other biomes to expand the understanding of canopy cover estimation using ATL08 data.

Biomass estimation derived from ATL08 data reported an average RMSE of 35.4% (standard deviation = ±26.1; R^2 = 0.71; RMSE = 35.35 Mg/ha; bias = 2.43 Mg/ha). These accuracy metrics, comparable to canopy metrics, exhibited variability across biomes and reference datasets. Approximately 72.9% of the biomes studied focused on five biomes: TrBrMoist, TeBrMix, TeCo, BoF, and Global. Among the global-scale studies, three have applied *ICESat-2* for biomass estimation [94], [41] and carbon stock assessment [96], reporting R^2 values ranging from 0.62 to 0.77.

Performance varied significantly in biomass studies, with TrBrMoist and TrBrDry showing superior results (RMSE <4.6%, n = 2) compared to TeBrMix, BoF, and MedF (RMSE >22.6%; n = 5). For instance (see Table 8), Neuenschwander et al. [97] and Varvia et al. [25] utilized ATL08 combined with ATL03 data (V004 and V005), leveraging advanced photon-counting algorithms and simulated data to generate reference datasets for biomass prediction in BoF. They reported RMSE values ranging from 26.9% to 64.0%, highlighting the challenges in sparsely wooded boreal ecosystems. By contrast, Nandy et al. [98] focused on TrBrMoist; integrating *ICESat-2* and *Sentinel-1* data achieved a significantly lower RMSE of 4.6% (R^2 = 0.83). Additionally, segment size was identified as a key factor influencing biomass assessment using ATL08 data [Figure 11(b)]. However, most studies used a 100-m segment size (n = 21), while only two studies used 30- and 90-m segment sizes for biomass estimation [Figure 11(e)].

Ten studies (8.8% of the 114 canopy-related articles) focused on ecological applications, such as LAI, carbon stock, forest age, and diversity. For LAI estimation, Qin et al. [99] generated high-resolution LAI maps by integrating ATL03 and ATL08 data with Copernicus datasets using machine learning algorithms, with random forest showing the best performance (R^2 of 0.9, RMSE% of 11%, and RMSE of 0.38 m^2/m^2 for TeBrMix). By contrast, Wang and Fang [100] integrated ATL08 data with Copernicus LAI maps for LAI estimation also on TeBrMix, yet with comparatively lower accuracy (R^2 of 0.63, RMSE% of 51.1%, and RMSE of 2.33 m^2/m^2). Forest age was another application; the integration of ATL08 data with a climate-driven model returned an R^2 of 0.67 and an RMSE of 12.79 years [71]. Yang et al. [101] utilized ATL03 and ATL08 datasets to estimate tree species diversity indices, achieving an R^2 of 0.54 for the Simpson index using *ICESat-2* alone and R^2 values of 0.64 and 0.54 for Shannon and species richness models, respectively, when integrating *ICESat-2* data with *Gaofen-1* panchromatic and multispectral sensor imagery.

From 293 studies, 33.8% (n = 99) integrated *ICESat-2* data with other remote sensing datasets for land and vegetation applications (Table 9). These studies validated *ICESat-2* data across different forest types and applications,

TABLE 9. EXAMPLES OF STUDIES FROM THE LITERATURE REVIEW ASSESSING THE PERFORMANCE OF INTEGRATED *ICESAT-2* DATA WITH OTHER ANCILLARY REMOTE SENSING DATASETS FOR WALL-TO-WALL LAND AND VEGETATION MAPPING APPLICATIONS.

AUTHOR	BIOME	TARGET	SEGMENT SIZE (M)	INTEGRATED DATASET	REFERENCE DATASET	PERFORMANCE
[114]	TeBrMix	Canopy height	ATL08 100	GEDI *Sentinel-1* *Sentinel-2* Terrain Climate	Field measurements	R^2: 0.64 RMSE: 16.1%
[107]	TrCo, TrGrSv, TeBrMix, TeCo, TeGrSv, FlGrSv, MedF, Deserts, Man	Canopy height	ATL08 20	Landsat LANDFIRE Topographic	ALS	R^2: 0.72 MAE: 23.3%
[115]	TeCo	Canopy cover	ATL08 100	Landsat NLCD land cover	NLCD tree canopy cover	R^2: 0.82 RMSE: 14.7%
[105]	TeBrMix	Canopy cover	ATL03; ATL08 100	Landsat *ALOS* DEM	Field measurements	R^2: 0.79 RMSE: 11%
[10]	MedF	Aboveground biomass	ATL08 (sim.) 100	GEDI NISAR	ALS	R^2: 0.63 RMSE: 49.9%
[108]	MedF	Aboveground biomass	ATL08 100	*Sentinel-1* *Sentinel-2* *ALOS-2*/PALSAR2	Field measurements	R^2: 0.63 RMSE: 28.5%
[99]	TrBrMoist	LAI	ATL03; ATL08 100	*Sentinel-1* *Sentinel-2*	N/A	R^2: 0.9 RMSE: 0.38 m^2/m^2

MAE: mean absolute error; NLCD: National Land Cover Database; *ALOS: Advanced Land Observing Satellite*; PALSAR: Phased Array L-band SAR.

showing varying performance based on dataset fusion, study scale, and target variables (Figure 11). These studies were implemented in all 15 biomes represented in the fusion-based studies [Figure 11(b)]. Of these, 80 out of 99 (80.8%) employed upscaling approaches to transition from coarse photon-counting footprints to wall-to-wall coverage. On the other hand, 67 out of 99 (67.7%) integrated *ICESat-2* data with other remote sensing datasets for forestry and ecological applications. Fourteen of 15 biomes were explored in canopy-related *ICESat-2* studies, especially TeBrMix, TrBrMoist, TeCo, and BoF (73.7%). An important observation is that all studies relied on open source datasets as wall-to-wall products are usually developed over large areas where open data are more accessible and consistent for large-scale mapping. Silva et al. [10] utilized a fusion approach that combined simulated ATL08 data, NISAR, and ALS to estimate aboveground biomass. Their results revealed an enhancement in accuracy featuring R^2 values between 0.61 and 0.63 and an RMSE of 115.86–130.57 Mg/ha. The bias in their study was relatively low, ranging from –16.25 to –7.01 Mg/ha. This highlights the advantage of integrating multiple remote sensing datasets for biomass estimation. Malambo and Popescu [107] mapped canopy height across the United States by fusing ATL08 data with Landsat, LANDFIRE, and topographic variables using a gradient-boosted regression model. Accuracy assessment with ALS achieved an overall R^2 of 0.72 and a mean absolute error (MAE) of 23.3%, with performance varying by biome. Guerra-Hernández et al. [108] used *ICESat-2*, *Sentinel-1*, and *Sentinel-2* to estimate large-scale aboveground biomass. Using random forest models, they achieved an R^2 of 0.63, an RMSE of 11.1 Mg ha^{-1} (RMSE% = 28.2%), and a bias of 0.03 Mg ha^{-1}. Several studies [109]–[113] have combined GEDI with *ICESat-2* data to assess forest canopy height [Figure 11(b) and (f)]. The R^2 across these investigations ranged from 0.55 to 0.67, while the RMSE varied between 2 and 8 m. The highest levels of error were observed in tropical and subtropical biomes.

DISCUSSION

From a systematic search of the research literature pertaining to the use of *ICEsat-2* for land and vegetation applications, as of December 2024, 293 peer-reviewed, published articles were identified and summarized according to application, data type, geographic domain, and methods employed. The synthesis of research exposes gaps, biases, and research opportunities. The following sections discuss the implication of the findings from the literature review and updates of the ICESat-2 mission regarding its land and vegetation applications.

CONSIDERATIONS ON CURRENT CAPABILITIES AND LIMITATIONS OF ICESAT-2 FOR LAND AND VEGETATION APPLICATIONS

The accurate terrain and canopy elevation retrieval at global scales enabled by *ICESat-2* is an exciting opportunity for land and vegetation applications. However, there are specific considerations regarding the capabilities—including both advantages and limitations—in the application of *ICESat-2* for vegetation research. The quantification of the vertical distribution of photons within the forest canopy provides invaluable information to inform estimates of biomass, canopy volume, forest structure, and species diversity [3], [100], [101]. The ability to extract estimates of terrain and canopy height in areas of high topographic relief is greatly improved over *ICESat* given *ICESat-2*'s 70-cm along-track photon detection. A key consideration and current limitation in the use of *ICESat-2* for vegetation applications is the observed difference in height and cover estimates among ecosystems. The photon-counting detection sensitivity of the ATLAS instrument on *ICESat-2* results in fewer photons reflected over land and even fewer over vegetated surfaces because of their lower reflectivity compared to snow and ice [116]. Further, the lower laser emission energy of the *ICESat-2* system leads to loss of the ground signal in areas of dense forest [3]. This reduction in point density creates a greater error and potential misclassification of photons returned from the understory as noise [5]. Zhang et al. [104] showed that canopy cover had a strong influence on the number of ground returns, with fewer ground returns as canopy cover increased.

In dense forests, such as those found in the tropics, the majority of photons returned emanate from the forest canopy, resulting in greater terrain and canopy height estimation error [56]. The distribution of these errors tends to be uniform and correlated with canopy height, suggesting potential error propagation that could be integrated into models or algorithms as a means of correction. In sparse cover, open systems such as savannas, discrimination between canopy returns and solar background noise becomes an issue [3]. Additionally, the dominance of low-stature and sparse vegetation in these ecosystems leads to a significant disparity in the spatial density of ground and canopy photons, with the high prevalence of ground photons limiting the accurate estimation of vegetation height [117]. To address this challenge, Li et al. [118] proposed a terrain-adaptive method that generates continuous terrain models, effectively removing dense ground photons and enhancing vegetation height retrieval accuracy. In fact, the proposed method achieved significantly better results, with derived vegetation heights showing an RMSE of 0.78 m, compared to the original ATL08, which had an RMSE of 4.26 m. Similarly, Wang et al. [119] developed a sectional photon denoising method for processing *ICESat-2* data in a sparsely forested region of China. This method significantly improved the correlation between the *ICESat-2*-reported canopy height (RH98) and the ALS-derived canopy height. Specifically, after modifying the original ATL08 product using their approach, they achieved a correlation of 0.82 and an RMSE of 3.52 m, compared to the original values of r = 0.6 and RMSE = 5.13 m. As such, while *ICESat-2* may be most suitable for use in boreal and temperate systems, it can also serve as a strong complement to instruments such as GEDI in the tropics, particularly for areas of secondary or degraded forest.

Differences in the strong and weak beams from *ICESat-2* and the way in which the instrument records the reflectance of photons create considerations for the use of day versus night retrievals. Moudrý et al. [120] evaluated the accuracy of *ICESat-2* terrain and canopy heights in the Czech Republic under varying instrument and environmental parameters and found that night acquisitions with a clear atmosphere resulted in lower RMSE errors for both terrain and canopy heights—a pattern also observed by Neuenschwander et al. [24] and Liu et al. [122]. Thus, current recommendations for accurate height and biomass retrievals emphasize the use of strong beam and/or night data [25], [76], [123]. Observed errors in the ATL08 estimated terrain and canopy heights are fundamentally due to either instrument limitations, such as low sampling rates, or challenges in photon classification and ground detection under complex canopy and terrain conditions. Malambo and Popescu [6] assessed the agreement of *ICESat-2* terrain and canopy heights over U.S. ecozones by comparing them to ALS data. They found that ATL08 terrain elevations overestimated ALS terrain elevations by, on average, 0.18 m (0.1%), while ATL08 canopy heights underestimated comparable ALS canopy heights by –1.71 m (15.9%). Their analysis by ecozones indicated that ATL08 canopy heights have a higher agreement with reference ALS in relatively dense canopy environments, such as conifers and broadleaf forests, than in sparse environments, such as temperate grasslands and savannas. They attributed differences in performance between ATL08 terrain and canopy heights over multiple ecozones to differences in photon sampling rates over terrain and canopy surfaces compounded with background noise in *ICESat-2* photon data and to the effectiveness of ATL08 algorithms in classifying photons.

To better demonstrate how uncertainty in ground surface detection impacts the accuracy of ATL08 canopy height estimates, a study by Pang et al. [125] revealed that the correlation between the original ATL08 canopy height estimates and ALS-derived canopy height models ranged from 0.3 to 0.56, with RMSE values between 4.49 and 11.71 m, across varied terrain and forest cover conditions. However, after incorporating ALS-derived DEM data into the ATL08 product to refine canopy height estimates, these values improved significantly, with correlation coefficients ranging from 0.7 to 0.94 and RMSE values between 1.32 and 3.23 m. These findings underscore the critical need for improved detection of ground photons in areas with complex terrain and dense forest cover to enhance the accuracy of canopy height estimates derived from *ICESat-2* data. As such, future improvements in photon classification over ecozones with varied canopy cover and vegetation heights could lead to improved agreement between ATL08 products and vegetation structure metrics. Figure 12 illustrates improvements in the ground finding from Release 005 to Release 006 of the ATL08 data product. It is anticipated that further improvements will be realized with Release 007 and subsequent releases of the data product.

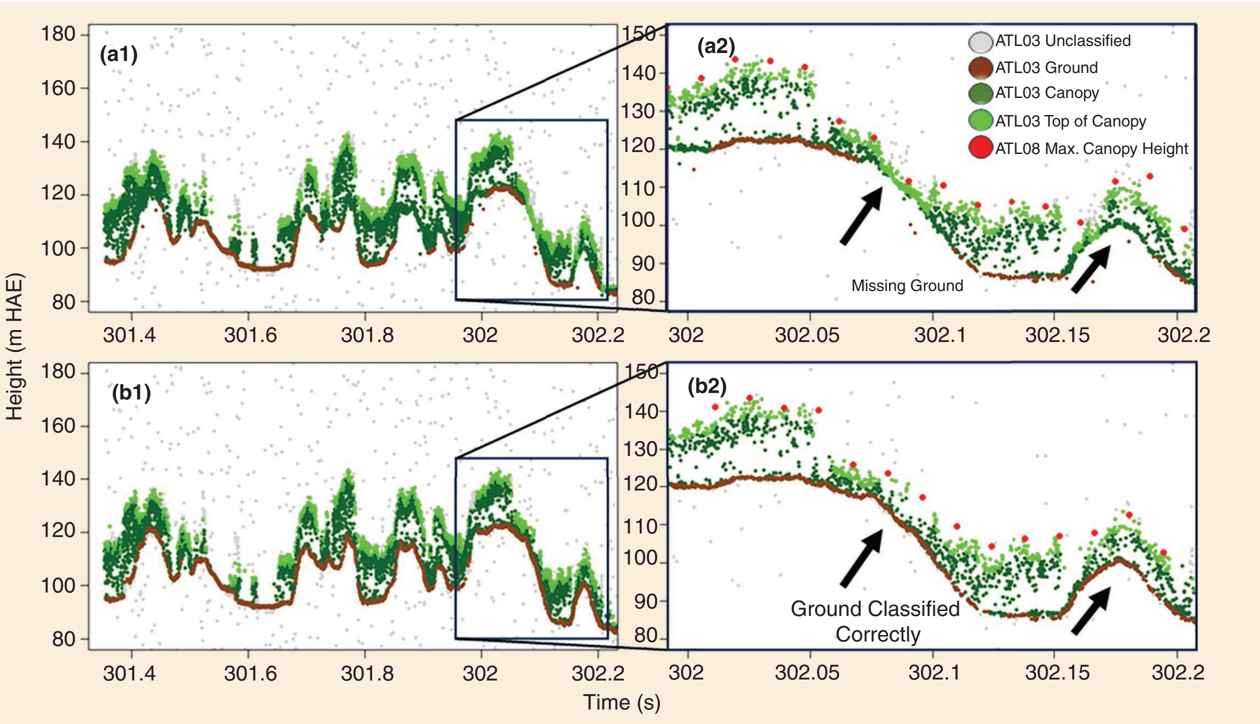

FIGURE 12. (a1), (b1) ATL08 Releases 005 and 006 labeled photons and maximum canopy height over Finland boreal forest illustrating (a2), (b2) improvements in the ground finding from Release 005 to Release 006 in areas with significant topographic relief variation.

The photon-counting approach of the ATLAS instrument results in the detection of many randomly distributed noise photons, necessitating reliable classification algorithms to parse out signals from noise. Further refinement of existing classification algorithms, such as Local Outlier Factor (LOF), LOF with rotating search area, DBSCAN, and quadtree isolation, or the development of new algorithms, are necessary to accelerate the use of *ICESat-2* for science applications and provide greater confidence in ATLAS data. Building on these efforts, recent studies have specifically addressed the challenges of noise filtering and photon classification [126]–[133]. For example, Tang et al. [127] introduced a Multilevel Auto-Adaptive Denoising (MLAD) algorithm to enhance the accuracy of forest structure parameter retrieval. By comparing MLAD with the Differential, Regressive, and Gaussian Adaptive Nearest Neighbor (DRAGAN) algorithm across various terrain slopes, vegetation coverages, and acquisition modes (strong versus weak beams), they demonstrated that MLAD significantly outperformed DRAGAN in retaining signal photons while effectively removing noise photons. A promising approach was proposed by Chen et al. [132], who developed a new multidimensional statistical algorithm based on a Gaussian mixture model (GMM) for photon noise removal. The authors highlighted two key advantages of the GMM algorithm. First, its adaptive classification eliminates the need for manual threshold determination, making the classification process more scientifically grounded and reducing the reliance on human input. Second, the use of multidimensional statistics allows the GMM algorithm to denoise using various statistical measures simultaneously. When compared with mainstream methods like DBSCAN and the *k*-nearest neighbors model, the results showed that the GMM method achieved a superior denoising performance. Also, demonstrating the potential of deep learning methods in enhancing photon denoising tasks, Qin et al. [128] proposed a novel CNN-based *ICESat-2* signal photon extraction method. The approach integrates the GoogLeNet model with a Convolutional Block Attention Module to improve the accuracy of signal photon extraction from *ICESat-2* cloud data. When comparing the terrain elevation results derived from this method with those obtained from the DBSCAN and the algorithm Ordering Points to Identify the Clustering Structure, the RMSE values were notably lower: 3.86, 4.98, and 10.52 m, respectively.

A limitation of *ICESat-2* (or any laser altimeter system) is the penetration of the laser energy through clouds to the surface. Laser pulses transmitted from spaceborne lidar systems are stretched because of multiple scattering effects caused by clouds, fog, and blowing snow, impacting altimetry measurements [134], [135]. *ICESat-2*'s green laser, however, can distinguish between clouds and aerosol constituents based on the backscatter characteristics of the laser energy and layer heights within the atmosphere, which are denoted in the cloud flag on the data product. (This is shown in detail in the Section "Considerations for ICESat-2 Product Improvements and Future Capabilities for Land and Vegetation Applications.") Furthermore, the ground surface is detectable in an atmosphere up to 0.75 optical depth. The data processing steps in the ATL08 algorithm employ several measures to eliminate perceived signal photons reflected from clouds such that they do not result in incorrect canopy or terrain heights. These steps eliminate the majority of potential blunders; yet, low-lying fog remains a challenge to the algorithm [22], [97]. For example, Figure 13(c) shows the surface detected even in the presence of fog. Although most fog/cloud photons were correctly labeled as noise, a few fog/cloud photons around the 50.15-s mark were mislabeled as canopy. This section of data, however, does have a multiple scatterer warning flag of 2, which indicates that significant atmospheric scattering is detected and it is recommended to utilize the parameter flags on the ATL08 data product.

Moudrý et al. [120] showed that the cloud cover flag was a significant predictor in explaining the number of canopy photons registered by *ICESat-2*. While several studies have employed quality flags to filter high-quality *ICESat-2* data segments—such as the cloud confidence flag [136], the multiple scattering warning flag [137], and the layer flag [120]—few have concentrated specifically on assessing how these atmospheric effects impact terrain and canopy height estimation accuracy [120], [24]. For instance, Palm et al. [138] recommended using the multiple scattering flag for nighttime acquisitions, whereas Moudrý et al. [120] found no direct correlation between the use of this flag and the number of ground photons or terrain accuracy. This underscores the need for further research to better evaluate the reliability of these flags under different conditions (e.g., nighttime versus daytime acquisitions and snow-covered versus nonsnow-covered environments) in identifying high-quality *ICESat-2* segments.

As described previously, the number of detected photons is contingent upon several parameters, including laser energy, atmospheric conditions, solar elevation, and surface reflectance. In Figure 13(a), it is apparent that the surface reflectance from the cleared forest is greater than that over the forest based upon the apparent background rate. Higher surface reflectance results in an increase of both signal and background photons. A change in the background rate can be a natural indicator of a change in either surface reflectance or reflectance from clouds in the atmosphere. In Figure 13(b), *ICESat-2* strong beams over a forested floodplain in Peru reveal the unique capability to detect water beneath the vegetation.

Although the original 100-m segment size of the ATL08 product is the one most commonly used by the scientific community, other segment sizes have been employed for canopy height estimation. For example, studies have used 20-m [61], [139], 30-m [97], and 90-m segments [140]. Other studies have tested the effects of varying segment sizes (e.g., 10–100 m) on the accuracy of canopy height and terrain elevation estimates [122], [125], [141], [142]. Overall, these studies concluded that increasing the segment size improves the accuracy of vegetation height and terrain elevation estimates. While most of these studies have been conducted in temperate and boreal forests, there is still a limited number of accuracy assessments for canopy and terrain height estimations across different segment sizes in semiarid ecosystems, which are characterized by low-stature and sparse vegetation [11]. Among the studies reviewed, only two specifically addressed the optimal segment size for retrieving LAI from *ICESat-2* data [67], [100]. For example, Wang and Fang [100] tested three different segment sizes (20, 100, and 200 m) and found that the highest correlation between *ICESat-2*-derived LAI and ALS-derived LAI occurred with a 200-m segment size in their study area. Therefore, there is still a need for more extensive validation efforts for both ATL08-derived terrain and canopy height retrievals as well as other vegetation structural metrics (e.g., LAI), at various segment sizes (e.g., 20, 30, and 100 m) across different ecozones, particularly in semiarid ecosystems.

Validating *ICESat-2* retrievals against data from other sources, such as ALS and terrestrial laser scanning or, alternatively, against other lidar spaceborne sensors like GEDI, is crucial for enhancing data accuracy and broadening its applications. The GEDI mission, for example, has been generating forest structure grid products, including canopy height and cover maps (Level 3 A) [143]. Although GEDI's coverage is limited to latitudes between 51.6° N and 51.6° S, it complements the ATL18 product and will serve as a reference for assessment once the product becomes available. Additionally, *ICESat-2* holds significant potential for applications focused on studying wildlife habitat, as demonstrated by previous research using GEDI data [144]. However, no *ICESat-2* studies on this topic have been found in the literature search. Beyond wildlife studies, *ICESat-2*'s

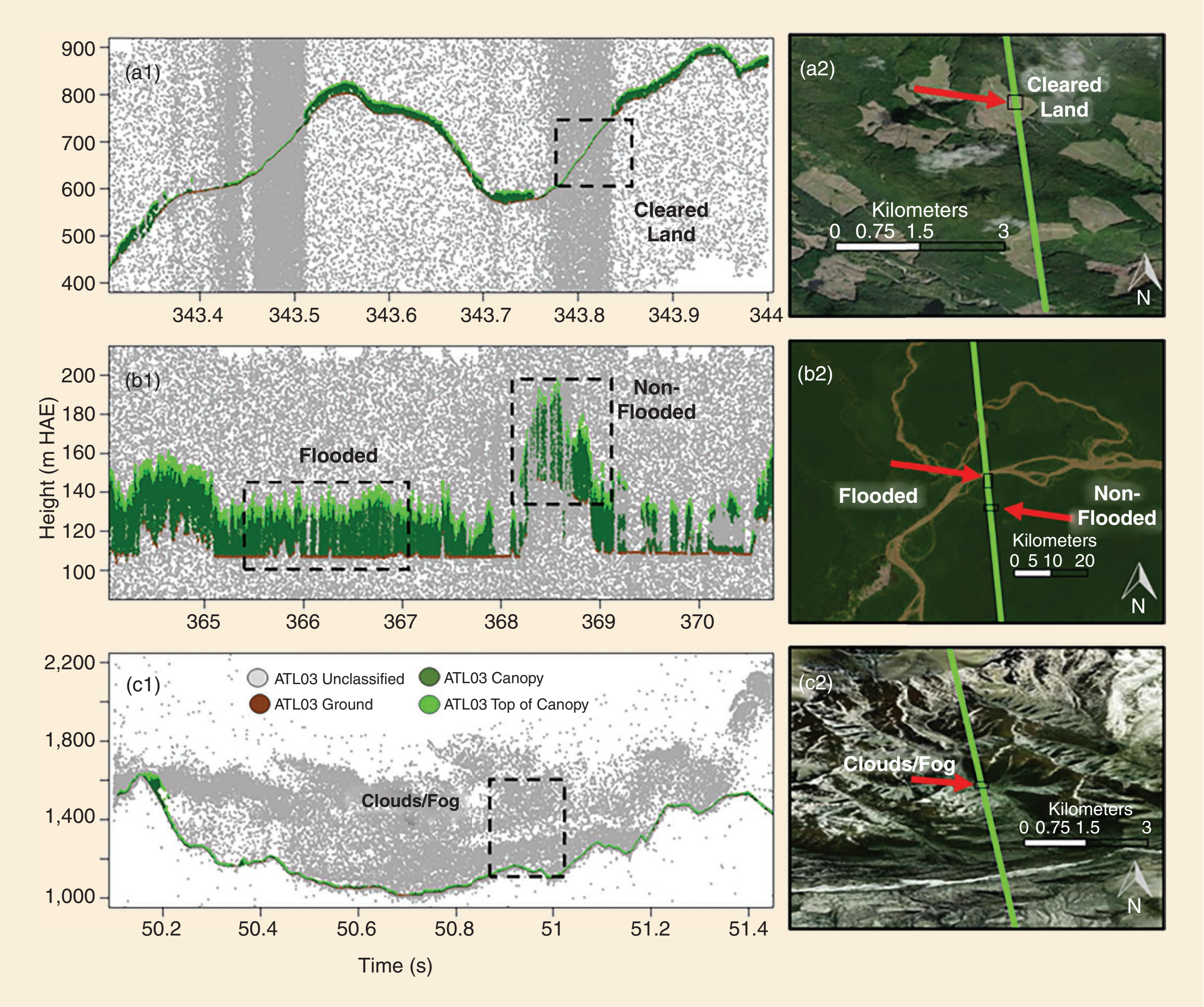

FIGURE 13. Examples of labeled ATL03 photon clouds over three sites. (a1)–(a2) *ICESat-2* strong beam passing through forest and cleared land, potentially also snow covered, in Washington State, United States (ATL03_20190228170214_09510202_006_02_gt1l). (b1)–(b2) *ICESat-2* strong beams over a forested floodplain in Peru (ATL03_20190410115035_01860314_005_01_gt1l). (c1)–(c2) *ICESat-2* detecting the surface in the presence of thin clouds/fog in Southeast Alaska (ATL03_20201118121426_08450903_006_01_gt1l).

ability to capture 3D vegetation structure also offers considerable insights for fire ecology applications. Several recent studies have begun to explore this potential, focusing on its use in burned forest classification [145], estimating carbon emissions from fire-induced biomass burning [58] and assessing post-fire changes in vegetation structure [11]. However, even though *ICESat-2* has a strong potential for characterizing critical fuel-related variables, such as canopy base height, canopy bulk density, and canopy fuel load—key inputs for fire simulators like FlamMap—these applications remain underexplored [14], [146]. Furthermore, *ICESat-2* showcases its versatility beyond forestry applications, revealing potential in urban environments, albeit within a limited scope. For instance, Zhao et al. [147] combined *ICESat-2* photons and Google Earth satellite images for building height extraction, while Li et al. [148] proposed a method for correcting *ICESat-2* terrain estimation within urban areas, utilizing a water pump deployment criterion aligned with the vertical contour of the terrain. Nonopen data are common in these applications since urban studies often require higher spatial resolution to accurately model structures. In such cases, commercial datasets, such as Pleiades and WorldView-2 imagery, have been integrated with *ICESat-2* to generate digital surface models and orthorectified images for detailed building footprint and height mapping [149]. In summary, these emerging applications reveal the versatility of *ICESat-2*, highlighting its potential for both natural and urban environments.

CONSIDERATIONS FOR ICESAT-2 PRODUCT IMPROVEMENTS AND FUTURE CAPABILITIES FOR LAND AND VEGETATION APPLICATIONS

The future of *ICESat-2* for land and vegetation applications is characterized by a multifaceted approach aimed at enhancing product quality and global-scale insights. There is anticipation for increasing the segment size of ATL08 data, allowing users to access terrain and vegetation heights at different scales, in addition to the 100-m segment. For instance, Feng et al. [22] compared ATL08 and Land, Vegetation, and Ice Sensor-derived terrain elevation and canopy height at a 30-m segment size in boreal forests and found RMSE and bias values of 3.19 m and 0.49 m for terrain elevation and an RMSE of 4.75 m and a bias of 0.88 m for canopy height. Figure 14 provides an example of ATL08-derived maximum canopy height computed at both 30- and 100-m segment sizes in southern forests in Florida. The potential benefits of a higher resolution ATL08 product, such as shifting from a 100-m to a 30-m segment size, could significantly enhance various applications in forestry, conservation, and climate studies. For example, finer resolution data on vegetation structure would improve the detection of small-scale disturbances, whether naturally occurring (e.g., insect outbreaks) or human-induced (e.g., changes in understory vegetation) [150], [151]. This increased resolution would also facilitate more detailed monitoring of ecosystem recovery patterns following such disturbances [93]. By delivering these high-resolution ATL08 products in a ready-to-use format, the scientific community would be able to focus more on conducting research and testing new applications rather than spending time on data preparation. This would not only accelerate the development of studies but also expand the potential of *ICESat-2* data to address key questions across a wider range of fields. Moreover, higher resolution ATL08 products would enhance validation efforts by improving the linkage between canopy height or derived aboveground biomass estimates and field-based or ALS-based measurements, thereby strengthening the accuracy of *ICESat-2* validation studies [22]. They would also enable more precise wall-to-wall mapping using 20–30-m pixel resolution satellite imagery [e.g., from *Sentinel-1*, *Sentinel-2*, *Landsat*, and *Advanced Land Observing Satellite* (*ALOS*)-*2*], facilitating the integration of *ICESat-2* data with passive optical imagery for more comprehensive land and vegetation monitoring [98], [108].

For further improvements, the ICESat-2 Science Team is also considering the integration of new parameters into the ATL08 data product, particularly those related to plant area index (PAI), plant area volume density (PAVD), and cover attributes [68]. These additions to the ATL08 product hold significant promise for applications in forestry and ecology, offering valuable tools to assess vegetation health and land cover dynamics. Beyond the proposed structural metrics like PAI and PAVD, the technological characteristics of *ICESat-2*—such as its small footprint size and high laser pulse repetition rate, which enable the generation of high-density point clouds and near-continuous sampling along the flight path [3]—highlight its potential for providing insights into the vertical complexity of vegetation. These features allow *ICESat-2* to capture the fine-scale structural variation that is essential for assessing vegetation vertical heterogeneity. A preliminary effort to derive this type of information from *ICESat-2* was presented by Yang et al. [101], who used statistical dispersion metrics (e.g., standard deviation and coefficient of variation) of percentile canopy heights within each ATL08 segment to characterize the vertical variation of vegetation. However, further research is needed to explore the feasibility of entropy-based metrics [152], [153], particularly using the photon-level data from the ATL03 product, to develop a novel vertical heterogeneity index for *ICESat-2*. This could boost new *ICESat-2* applications for vegetation structure heterogeneity assessments and enhance our understanding of ecosystem complexity at a large scale.

One notable advancement is the production of gridded products to provide a comprehensive understanding of vegetation structure across the globe, exemplified by ATL18, which focuses on gridded canopy height at a global scale at 1-km spatial resolution. Such developments are crucial for uptake by the land surface modeling community, which requires regional and global gridded products to parameterize vegetation within its simulations of soil–vegetation–atmosphere interactions [154] as well as for carbon stock and flux assessments [89]. Another pivotal aspect of *ICESat-2*'s future development is the improvements in pointing control, from the initial goal of 45 m to ~3 m, and in geolocation accuracy, reducing errors from ~5 m to about 2 m [19]. These advancements, combined with near-repeat-track retrievals, will significantly enhance the development of change-detection methodologies capable of directly capturing vegetation structural changes in response to natural and human-induced disturbances. This will enable more precise and continuous monitoring of land and vegetation changes and will improve *ICESat-2*'s capability of detecting and monitoring disturbances, such as those caused by fires [11]. This dynamic capability positions *ICESat-2* as a crucial asset in ongoing efforts to understand and respond to environmental transformations on a global scale.

SYNERGIES OF ICESAT-2 WITH EXISTING AND UPCOMING EARTH OBSERVATION MISSIONS FOR LAND AND VEGETATION APPLICATIONS

There are many opportunities for synergy between *ICESat-2* and other current and planned spaceborne remote sensing missions, creating an exciting frontier for *ICESat-2* applications in terrestrial environments. For instance, as presented in the section "Considerations for ICESat-2 Product Improvements and Future Capabilities for Land and Vegetation Applications," synergistic opportunities between *ICESat-2* and other passive optical and SAR sensors (e.g., L8, *Sentinel-1*'s C/2A, *ALOS-2*'s Phased Array L-band SAR (PALSAR), the Moderate Resolution Imaging Spectroradiometer, and PlanetScope) have already been explored to inform mapping aboveground biomass [10], [54], [60], [108], carbon emissions from fire [58], burned-area extent and impacts [155], and dryland vegetation cover [156]. ECOSTRESS, a sensor aboard the International Space Station that provides highly accurate measurements of plant temperature, has been paired with structural data from GEDI to map evapotranspiration, quantifying the role that forest structure plays in the photosynthetic process [157], [158]. The Orbiting Carbon Observatory 3 (OCO-3) from NASA provides measurements of solar-induced fluorescence and column CO_2, allowing for the estimation of photosynthesis from space. Expanded use of OCO-3 and ECOSTRESS with sensors such as *ICESat-2* will help to answer fundamental questions

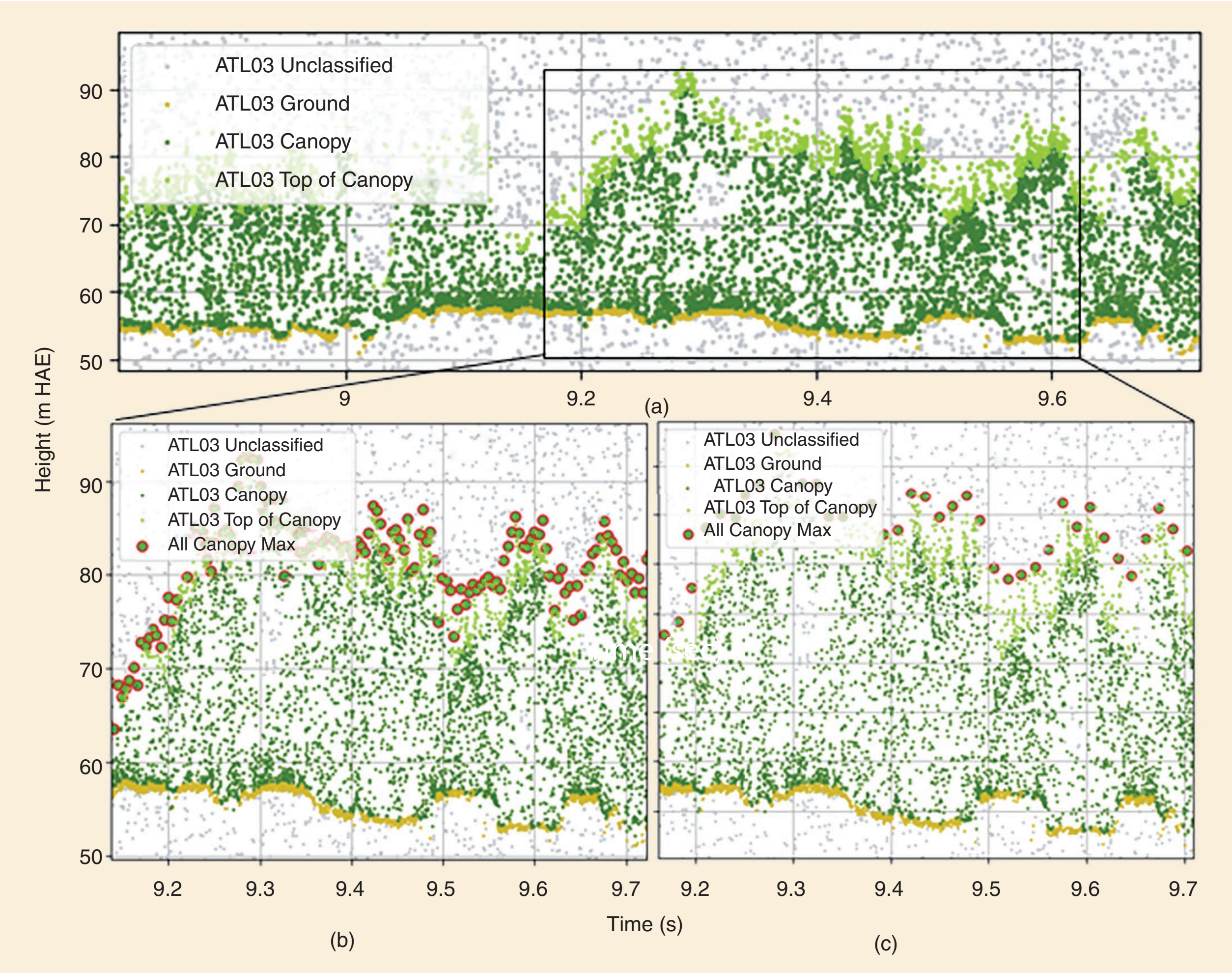

FIGURE 14. (a) Labeled photons over longleaf pine forests in Florida and an example of top canopy height computed at (b) 30-m and (c) 100-m segment sizes.

regarding plant function, including the role of structure to mediate production and transpiration.

Future and upcoming missions from NASA, the ESA, and others, including ISRO, portend even greater possibilities in the future. Launched in July 2025, NISAR provides yet another means of quantifying structure from space, further increasing spatial and temporal coverage. A framework for fusing *ICESat-2*, GEDI, and NISAR as an approach to more accurately derive aboveground biomass was investigated by Silva et al. [10] using simulated *ICESat-2* and GEDI data from ALS data. The authors showed that fusion approaches that combined information from all three sensors more closely approximated reference aboveground biomass estimates, demonstrating the potential for increased geographic coverage of mapped biomass products. In addition to NISAR, the ESA's BIOMASS mission satellite, launched in April 2025, will be another SAR instrument, the first P-band SAR instrument in space. BIOMASS has a specific goal of providing global biomass estimates for at least five years post-launch. Both GEDI and *ICESat-2* data and data products will serve to help guide algorithm development for BIOMASS as a calibration/validation dataset but are also natural synergies for BIOMASS, potentially allowing for a consistent, globally mapped biomass product when all are merged [159].

Exciting synergy opportunities exist between *ICESat-2* and NASA's upcoming Surface Biology and Geology (SBG) mission. The SBG mission seeks to measure biological, physical, chemical, and mineralogical features of Earth's surface using a multisensor approach including a visible-to-shortwave infrared (VSWIR) spectrometer and a multichannel thermal radiometer on a separate platform, slated to launch in 2027–2028 [160], [161]. The mission also involves cooperation among multiple agencies from many nations. Synergistic missions include the European Union and ESA Copernicus Hyperspectral Imaging Mission for the Environment, which supports two independent, polar-orbiting VSWIR imaging spectrometers [83], the ESA's Copernicus Land Surface Temperature Monitoring (https://www.eoportal.org/satellite-missions/lstm) mission's two polar-orbiting thermal imagers, and the Thermal Infrared Imaging Satellite for High-Resolution Natural Resource Assessment (https://trishna.cnes.fr/en/trishna-0)—a National Center for Space Studies and ISRO cooperative mission supporting a polar-orbiting thermal imager [161].

The abundance and diversity of sensors coupled with advances in scientific computing, increased revisit capability, and longer data collection times create the potential for wall-to-wall multidimensional (3D and 4D) mapping of process, functional, and structural change [95]. This is further reinforced by NASA's recently selected Earth Dynamics Geodetic Explorer, which will provide next-generation spaceborne lidar observations with improved coverage and enhanced spatial and vertical precision. The fusion of various data streams will help to fill spatial and temporal gaps, providing near-global coverage [121].

GAPS IN CURRENT KNOWLEDGE AND TOPICS FOR FUTURE RESEARCH

Despite the large body of research that focused on ATL03 noise filtering and photon classification, there is a lack of joint efforts for which the various new algorithms would be tested together in different types of forests, ranging from dense tropical rainforests to sparsely wooded boreal forests and savannas. It is unlikely that a single method with a single set of parameters would outperform its alternatives because, in addition to vegetation type, for example, terrain topography, time of day, and presence of snow complicate the analysis [21], [25]. However, currently most of the new filtering algorithms have not been validated beyond their original datasets, and their source codes might also not be available for the public. Introduction of these methods for wider use therefore requires additional efforts. There is also little research on the use of *ICESat-2* for land cover types that are vegetated but not forested, such as agricultural fields and rangelands, although vegetation heights can be rather large in such areas. Future research should focus on testing different filtering algorithms across diverse forest types and land cover, supported by the availability of open repositories for source codes. These are essential to ensure reproducibility, enable fair comparisons among methods, and expand the applicability of these algorithms to other areas.

THIS REVIEW EXAMINED 293 PEER-REVIEWED ARTICLES THAT USED *ICESAT-2* DATA FOR LAND AND VEGETATION APPLICATIONS, PROVIDING AN OVERVIEW OF NASA'S ICESAT-2 MISSION AND A GLOBAL SYNTHESIS OF RESEARCH TRENDS, METHODS, AND FINDINGS.

Estimations of forest attributes that cannot be obtained directly from the photon data, such as aboveground biomass, require the use of simulations [68], [97] or statistical proxy models [25], [108] in the linking of *ICESat-2* predictors with field measurements. Both methods have their own limitations: simulations inherently rely on the validity of the simulations, while proxy models require long modeling chains that can lead to saturation of predicted forest attributes. Currently, there is a lack of research that would compare these two approaches in different situations. Therefore, we reinforce the importance of making datasets openly available to support consistent model assessment and development, and we highlight the need for greater future research efforts in biomes with limited reference data.

ICESat-2 data are best suited for large area applications, which introduces limitations to its use. The limited availability of ALS data required for validating the photon filtering and applied models is limited, which means that both filtering methods and modeling techniques should be validated for large areas. This requires both stratification by forest type and the introduction of more transferable models that include, e.g., climatic variables as predictors. Forest inventories also require estimating the uncertainty of predictions, and although some novel methodologies for this have been recently published [140], [124], the estimated model-based uncertainties rely on assumptions that the applied models are valid in the entire area of application. To address these issues, the initiation of joint efforts aiming at validating continental-scale estimations with pooled reference datasets would be direly needed.

CONCLUSION

This review examined 293 peer-reviewed articles that used *ICESat-2* data for land and vegetation applications, providing an overview of NASA's ICESat-2 mission and a global synthesis of research trends, methods, and findings. These applications span forest structure analysis, terrain modeling, and ecological monitoring, underscoring the growing interest of the scientific community in leveraging *ICESat-2*'s capabilities for terrestrial Earth observation. We highlighted the spatial and thematic distribution of studies, showing an uneven distribution of studies across terrestrial biomes, and a broad range of analytical approaches, including both traditional parametric models and more recent advances in machine learning and data fusion. While the mission has proven valuable for characterizing vegetation structure and terrain features, limitations remain in complex environments and in the absence of standardized processing approaches. Additionally, certain domains, such as nonforest vegetation, fire ecology, urban landscapes, and habitat assessments, remain underexplored, highlighting opportunities to broaden the mission's impact.

ICESat-2'S CONTRIBUTION WILL EXPAND THROUGH ITS INTEGRATION WITH OTHER COMPLEMENTARY SPACEBORNE MISSIONS SUCH AS GEDI, NISAR, AND BIOMASS.

Moving forward, *ICESat-2*'s contribution will expand through its integration with other complementary spaceborne missions, such as GEDI, NISAR, and BIOMASS. The fusion of these promising datasets, including photon-counting lidar, waveform lidar, and high-resolution radar data, will enable more consistent and spatially continuous estimates of canopy height, biomass, and ecosystem structure. These cross-mission synergies will improve temporal continuity and enhance monitoring frameworks for quantifying forest change, carbon dynamics, and climate-driven disturbances at global scales.

Altogether, *ICESat-2* continues to perform beyond ice, offering transformative insights and opportunities for terrestrial ecosystem science.

ACKNOWLEDGMENT

This study was primarily funded through NASA's grants (ICESat-2, 80NSSC23K0941), Carbon Monitoring System (CMS, grant 80NSSC23K1257), Commercial Smallsat Data Scientific Analysis (CSDSA, grant 80NSSC24K0055), and the McIntire -Stennis Program, University of Florida (Accession No. 7005758). Amy Neuenschwander was supported through grants from NASA's ICESat-2 as well (80NSSC23K0976 and 80NSSC20K0965). Lauri Korhonen was supported by the National Research Council of Finland (grant 363927). Veraldo Liesenberg was supported by the Brazilian National Council for Scientific and Technological Development (grant 312263/2025-2). We thank Lisar Kaser for providing the ICESat-2 data access and download statistics used in this study. Inacio T. Bueno is the corresponding author.

Author contributions are as follows:

1) C. A. Silva: Conceptualization, methodology; formal analysis; funding acquisition; investigation; methodology; project administration; resources; supervision; visualization; writing, original draft; writing, review and editing
2) A. Neuenschwander: Conceptualization; formal analysis; methodology; visualization; writing, review and editing
3) C. Hamamura: Data curation; formal analysis; investigation; software; visualization; writing, review and editing
4) S. Godinho: Data curation; writing, review and editing
5) K. M. Brock: Data curation; writing, review and editing
6) L. Malambo: Writing, review and editing
7) L. Narine: Data curation; writing, review and editing
8) J. W. Atkins: Writing, review and editing
9) J. Borak: Data curation
10) S. Popescu: Writing, review and editing
11) I. T. Bueno: Data curation; validation; visualization; writing, review and editing
12) L. B. Rezende: Data curation; writing, review and editing
13) G. B. Santoro: Data curation; writing, review and editing
14) A. P. Dalla Corte: Writing, review and editing
15) C. I. A. Diaz: Data curation; writing, review and editing
16) N. Mashhadi: Data curation; writing, review and editing
17) A. Cardil: Writing, review and editing
18) A. T. Hudak: Writing, review and editing
19) L. Korhonen: Writing, review and editing
20) A. Sharma: Writing, review and editing
21) J. B. Cannon: Writing, review and editing
22) M. Mohan: Writing, review and editing
23) W. S. W. Mohd Hafar: Writing, review and editing
24) V. Liesenberg: Writing, review and editing
25) C. Klauberg: Writing, review and editing.

AUTHOR INFORMATION

Carlos Alberto Silva (c.silva@ufl.edu) is with Forest Biometrics, Remote Sensing and Artificial Intelligence Laboratory (SilvaLab), School of Forest, Fisheries, and Geomatics Sciences, University of Florida, Gainesville, FL 32611 USA. He is a Member of IEEE.

Amy Neuenschwander (amy@csr.utexas.edu) is with the 3D Geospatial Laboratory, Center for Space Research, University of Texas at Austin, Austin, TX 78759 USA.

Caio Hamamura (hamamura.caio@ifsp.edu.br) is with the Federal Institute of Education, Science and Technology of São Paulo, Capivari, SP 13365-010, Brazil.

Sérgio Godinho (sgodinho@uevora.pt) is with the Mediterranean Institute for Agriculture, Environment and Development and CHANGE – Global Change and Sustainability Institute, Instituto de Investigação e Formação Avançada, Universidade de Évora, 7006-554 Évora, Portugal, and the Earth Remote Sensing Laboratory, University of Évora, 7000-671 Évora, Portugal.

Kody M. Brock (kody.brock@ufl.edu) is with Forest Biometrics, Remote Sensing and Artificial Intelligence Laboratory (SilvaLab), School of Forest, Fisheries, and Geomatics Sciences, University of Florida, Gainesville, FL 32611 USA.

Lonesome Malambo (mmoonga@tamu.edu) is with the Department of Ecology and Conservation Biology, Texas A&M University, College Station, TX 77843 USA.

Lana Narine (lln0005@auburn.edu) is with the College of Forestry, Wildlife and Environment, Auburn University, Auburn, AL 36849 USA.

Jeff W. Atkins (jwatkins6@vcu.edu) is with Virginia Commonwealth University, Richmond, VA 23284 USA.

Jordan S. Borak (jborak@umd.edu) is with the Earth System Science Interdisciplinary Center, University of Maryland, College Park, MD 20740 USA, and the NASA Goddard Space Flight Center, Greenbelt, MD 20771 USA.

Sorin Popescu (s-popescu@tamu.edu) is with the Department of Ecology and Conservation Biology, Texas A&M University, College Station, TX 77843 USA.

Inacio T. Bueno (ithomazbueno@ufl.edu) is with Forest Biometrics, Remote Sensing and Artificial Intelligence Laboratory (SilvaLab), School of Forest, Fisheries, and Geomatics Sciences, University of Florida, Gainesville, FL 32611 USA.

Lucas Bielak Rezende (bielak@ufpr.br) is with the Department of Forest Science, Federal University of Paraná, Curitiba, PR 80060-000, Brazil.

Giulio Brossi Santoro (gb.santoro@ufl.edu) is with Forest Biometrics, Remote Sensing and Artificial Intelligence Laboratory (SilvaLab), School of Forest, Fisheries, and Geomatics Sciences, University of Florida, Gainesville, FL 32611 USA.

Ana Paula Dalla Corte (anacorte@ufpr.br) is with the Department of Forest Science, Federal University of Paraná, Curitiba, PR 80060-000, Brazil.

Cesar Ivan Alvitez Diaz (c.alvitesdiaz@ufl.edu) is with Forest Biometrics, Remote Sensing and Artificial Intelligence Laboratory (SilvaLab), School of Forest, Fisheries, and Geomatics Sciences, University of Florida, Gainesville, FL 32611 USA.

Nooshin Mashhadi (nmashhad@ualberta.ca) is with the Department of Earth and Atmospheric Sciences, University of Alberta, Edmonton, AB T6G 2R3, Canada.

Adrián Cardil (adriancardil@gmail.com) is with the Department of Agricultural and Forest Sciences and Engineering, University of Lleida, 25198 Lleida, Spain.

Andrew T. Hudak (andrew.hudak@usda.gov) is with the USDA Forest Service Rocky Mountain Research Station, Moscow, ID 83843 USA.

Lauri Korhonen (lauri.korhonen@uef.fi) is with the University of Eastern Finland, School of Forest Sciences, 80101 Joensuu, Finland.

Ajay Sharma (azs0365@auburn.edu) is with the College of Forestry, Wildlife and Environment, Auburn University, Auburn, AL 36849 USA.

Jeffery B. Cannon (jeffery.cannon@jonesctr.org) is with the Jones Center at Ichauway, Newton, GA 39870-8522 USA.

Midhun Mohan (mikey@ecoresolve.eco) is with Ecoresolve, San Francisco, CA 94105 USA.

Wan Shafrina Wan Mohd Jafar (wanshafrina@ukm.edu.my) is with the Earth Observation Centre, Institute of Climate Change, Universiti Kebangsaan Malaysia, Bangi 43600, Selangor, Malaysia.

Veraldo Liesenberg (veraldo.liesenberg@udesc.br) is with the Department of Forest Engineering, Santa Catarina State University, Lages, SC 88520-000, Brazil.

Carine Klauberg (carine.klaubergs@ufl.edu) is with Forest Biometrics, Remote Sensing and Artificial Intelligence Laboratory (SilvaLab), School of Forest, Fisheries, and Geomatics Sciences, University of Florida, Gainesville, FL 32611 USA.

REFERENCES

[1] T. Markus et al., “The Ice, Cloud, and land Elevation Satellite-2 (ICESat-2): Science requirements, concept, and implementation,” *Remote Sens. Environ.*, vol. 190, pp. 260–273, Mar. 2017, doi: 10.1016/j.rse.2016.12.029.

[2] T. A. Neumann et al., “The Ice, Cloud, and Land Elevation Satellite – 2 mission: A global geolocated photon product derived from the Advanced Topographic Laser Altimeter System,” *Remote Sens. Environ.*, vol. 233, Nov. 2019, Art. no. 111325, doi: 10.1016/j.rse.2019.111325.

[3] A. Neuenschwander and K. Pitts, “The ATL08 land and vegetation product for the ICESat-2 Mission,” *Remote Sens. Environ.*, vol. 221, pp. 247–259, Feb. 2019, doi: 10.1016/j.rse.2018.11.005.

[4] L. A. Magruder, K. M. Brunt, and M. Alonzo, “Early ICESat-2 on-orbit geolocation validation using ground-based corner cube retro-reflectors,” *Remote Sens.*, vol. 12, no. 21, 2020, Art. no. 3653, doi: 10.3390/rs12213653.

[5] L. He, Y. Pang, Z. Zhang, X. Liang, and B. Chen, “ICESat-2 data classification and estimation of terrain height and canopy height,” *Int. J. Appl. Earth Obs. Geoinf.*, vol. 118, Apr. 2023, Art. no. 103233, doi: 10.1016/j.jag.2023.103233.

[6] L. Malambo and S. C. Popescu, “Assessing the agreement of ICESat-2 terrain and canopy height with airborne lidar over US

ecozones," *Remote Sens. Environ.*, vol. 266, Dec. 2021, Art. no. 112711, doi: 10.1016/j.rse.2021.112711.

[7] L. Duncanson et al., "Biomass estimation from simulated GEDI, ICESat-2 and NISAR across environmental gradients in Sonoma County, California," *Remote Sens. Environ.*, vol. 242, Jun. 2020, Art. no. 111779, doi: 10.1016/j.rse.2020.111779.

[8] P. M. Montesano et al., "The uncertainty of biomass estimates from modeled ICESat-2 returns across a boreal forest gradient," *Remote Sens. Environ.*, vol. 158, pp. 95–109, Mar. 2015, doi: 10.1016/j.rse.2014.10.029.

[9] L. L. Narine, S. C. Popescu, and L. Malambo, "Using ICESat-2 to estimate and map forest aboveground biomass: A first example," *Remote Sens.*, vol. 12, no. 11, 2020, Art. no. 1824, doi: 10.3390/rs12111824.

[10] C. A. Silva et al., "Fusing simulated GEDI, ICESat-2 and NISAR data for regional aboveground biomass mapping," *Remote Sens. Environ.*, vol. 253, Feb. 2021, Art. no. 112234, doi: 10.1016/j.rse.2020.112234.

[11] V. S. Konduri, D. C. Morton, and N. Andela, "Tracking changes in vegetation structure following fire in the Cerrado biome using ICESat-2," *J. Geophys. Res. Biogeosci.*, vol. 128, no. 5, 2023, Art. no. e2022JG007046, doi: 10.1029/2022JG007046.

[12] J. Cheng et al., "Satellite and UAV-based remote sensing for assessing the flooding risk from Tibetan lake expansion and optimizing the village relocation site," *Sci. Total Environ.*, vol. 802, Jan. 2022, Art. no. 149928, doi: 10.1016/j.scitotenv.2021.149928.

[13] C. Alvites, M. Marchetti, B. Lasserre, and G. Santopuoli, "LiDAR as a tool for assessing timber assortments: A systematic literature review," *Remote Sens.*, vol. 14, no. 18, 2022, Art. no. 4466, doi: 10.3390/rs14184466.

[14] M. E. Brown, S. D. Arias, and M. Chesnes, "Review of ICESat and ICESat-2 literature to enhance applications discovery," *Remote Sens. Appl. Soc. Environ.*, vol. 29, Jan. 2023, Art. no. 100874, doi: 10.1016/j.rsase.2022.100874.

[15] B. E. Schutz, H. J. Zwally, C. A. Shuman, D. Hancock, and J. P. DiMarzio, "Overview of the ICESat mission," *Geophys. Res. Lett.*, vol. 32, no. 21, 2005, doi: 10.1029/2005GL024009.

[16] R. Dubayah et al., "The global ecosystem dynamics investigation: High-resolution laser ranging of the Earth's forests and topography," *Sci. Remote Sens.*, vol. 1, Jun. 2020, Art. no. 100002, doi: 10.1016/j.srs.2020.100002.

[17] P. A. Rosen et al., "The NASA-ISRO SAR mission - An international space partnership for science and societal benefit," in *Proc. IEEE Radar Conf. (RadarCon)*, 2015, pp. 1610–1613, doi: 10.1109/RADAR.2015.7131255.

[18] S. Quegan et al., "The European Space Agency BIOMASS mission: Measuring forest above-ground biomass from space," *Remote Sens. Environ.*, vol. 227, pp. 44–60, Jun. 2019, doi: 10.1016/j.rse.2019.03.032.

[19] S. B. Luthcke et al., "ICESat-2 pointing calibration and geolocation performance," *Earth Space Sci.*, vol. 8, no. 3, 2021, Art. no. e2020EA001494, doi: 10.1029/2020EA001494.

[20] A. Gibbons, T. Neumann, D. Hancock, K. Harbeck, and J. Lee, "On-orbit radiometric performance on ICESat-2," *Earth Space Sci.*, vol. 8, no. 10, 2021, Art. no. e2020EA001503, doi: 10.1029/2020EA001503.

[21] A. Neuenschwander, L. Magruder, E. Guenther, S. Hancock, and M. Purslow, "Radiometric assessment of ICESat-2 over vegetated surfaces," *Remote Sens.*, vol. 14, no. 3, 2022, Art. no. 787, doi: 10.3390/rs14030787.

[22] T. Feng et al., "A systematic evaluation of multi-resolution ICESat-2 ATL08 terrain and canopy heights in boreal forests," *Remote Sens. Environ.*, vol. 291, Jun. 2023, Art. no. 113570, doi: 10.1016/j.rse.2023.113570.

[23] D. Entekhabi et al., "The Soil Moisture Active Passive (SMAP) mission," *Proc. IEEE*, vol. 98, no. 5, pp. 704–716, May 2010, doi: 10.1109/JPROC.2010.2043918.

[24] A. Neuenschwander, E. Guenther, J. C. White, L. Duncanson, and P. Montesano, "Validation of ICESat-2 terrain and canopy heights in boreal forests," *Remote Sens. Environ.*, vol. 251, Dec. 2020, Art. no. 112110, doi: 10.1016/j.rse.2020.112110.

[25] P. Varvia et al., "How to consider the effects of time of day, beam strength, and snow cover in ICESat-2 based estimation of boreal forest biomass?" *Remote Sens. Environ.*, vol. 280, Oct. 2022, Art. no. 113174, doi: 10.1016/j.rse.2022.113174.

[26] B. Fortner, "HDF: The hierarchical data format," *Dr Dobb's J. Softw. Tools Prof Program*, vol. 23, no. 5, p. 42, 1998.

[27] L. Malambo and S. Popescu, "PhotonLabeler: An inter-disciplinary platform for visual interpretation and labeling of ICESat-2 geolocated photon data," *Remote Sens.*, vol. 12, no. 19, 2020, Art. no. 3168, doi: 10.3390/rs12193168.

[28] A. L. Neuenschwander and L. A. Magruder, "PhoREAL: Increasing spatial and temporal data accessibly of ICESat-2 through open-source Python repository," in *Proc. Laser Radar Technol. Appl. XXVIII*, 2023, p. 95–101, doi: 10.1117/12.2667098.

[29] D. Shean et al., "SlideRule: Enabling rapid, scalable, open science for the NASA ICESat-2 mission and beyond," *J. Open Source Softw.*, vol. 8, no. 81, 2023, Art. no. 4982, doi: 10.21105/joss.04982.

[30] S. J. S. Khalsa et al., "OpenAltimetry - Rapid analysis and visualization of Spaceborne altimeter data," *Earth Sci. Inf.*, vol. 15, no. 3, pp. 1471–1480, 2022, doi: 10.1007/s12145-020-00520-2.

[31] B. Silva and L. G. Lopes, "A software tool for ICESat and ICESat-2 laser altimetry data processing, analysis, and visualization: Description, features, and usage," *Software*, vol. 3, no. 3, pp. 380–410, 2024, doi: 10.3390/software3030020.

[32] J. Scheick et al., "icepyx: Querying, obtaining, analyzing, and manipulating ICESat-2 datasets," *J. Open Source Softw.*, vol. 8, no. 84, 2023, Art. no. 4912, doi: 10.21105/joss.04912.

[33] L. Lopez, A. Barrett, A. E. Steiker, J. Scheick, J. S. S. Lowndes, and E. Robinson, "A Python package to search and access NASA earth science data," presented at the AGU Fall Meeting, Chicago, IL, USA, Dec. 12–16, 2022, id. IN22C-0318.

[34] L. Mouselimis, 2024, "IceSat2R: ICESat-2 Altimeter Data Using R," R Packag, version 1.0.6, doi: 10.32614/CRAN.package.IceSat2R.

[35] C. A. Silva and C. Hamamura. "ICESat2VegR: An R package for NASA's ice, cloud, and elevation satellite (ICESat-2) data processing and visualization for land and vegetation applications." GitHub. [Online]. Available: https://github.com/carlos-alberto-silva/ICESat2VegR

[36] C. A. Silva and C. Hamamura, "ICESat2VegR: An R Package for NASA's Ice, Cloud, and Elevation Satellite (ICESat-2) data processing and visualization for land and vegetation applications," 2024.

[37] L. Malambo, "xATLy: Extending ICESat-2 ATL03 and ATL08 products for land and vegetation analyses," 2023. Accessed: Nov. 11, 2023. [Online]. Available: https://github.com/Oht0nger/xATLy/releases/tag/1.0.0

[38] A. Liberati et al., "The PRISMA statement for reporting systematic reviews and meta-analyses of studies that evaluate health care interventions: Explanation and elaboration," *PLoS Med.*, vol. 6, no. 7, 2009, Art. no. e1000100, doi: 10.1371/journal.pmed.1000100.

[39] D. Moher, A. Liberati, J. Tetzlaff, and D. G. Altman, "Preferred reporting items for systematic reviews and meta-analyses: The PRISMA statement," *PLoS Med.*, vol. 6, no. 7, 2009, Art. no. e1000097, doi: 10.1371/journal.pmed.1000097.

[40] R. Vernimmen, A. Hooijer, and M. Pronk, "New ICESat-2 satellite LiDAR data allow first global lowland DTM suitable for accurate coastal flood risk assessment," *Remote Sens.*, vol. 12, no. 17, 2020, Art. no. 2827, doi: 10.3390/rs12172827.

[41] C. Vittucci, L. Guerriero, and P. Ferrazzoli, "Influence of vegetation height, plant area index, and forest intactness on SMOS L-VOD, for different seasons and latitude ranges," *IEEE Trans. Geosci. Remote Sens.*, vol. 61, pp. 1–11, 2023, doi: 10.1109/TGRS.2023.3299529.

[42] W. Abdalati et al., "The ICESat-2 laser altimetry mission," *Proc. IEEE*, vol. 98, no. 5, pp. 735–751, May 2010, doi: 10.1109/JPROC.2009.2034765.

[43] M. McGill, T. Markus, V. S. Scott, and T. Neumann, "The Multiple Altimeter Beam Experimental Lidar (MABEL): An airborne simulator for the ICESat-2 mission," *J. Atmos. Ocean. Technol.*, vol. 30, no. 2, pp. 345–352, 2013, doi: 10.1175/JTECH-D-12-00076.1.

[44] J. Zhang and J. Kerekes, "An adaptive density-based model for extracting surface returns from photon-counting laser altimeter data," *IEEE Geosci. Remote Sens. Lett.*, vol. 12, no. 4, pp. 726–730, Apr. 2015, doi: 10.1109/LGRS.2014.2360367.

[45] U. C. Herzfeld et al., "Algorithm for detection of ground and canopy cover in micropulse photon-counting lidar altimeter data in preparation for the ICESat-2 mission," *IEEE Trans. Geosci. Remote Sens.*, vol. 52, no. 4, pp. 2109–2125, Apr. 2014, doi: 10.1109/TGRS.2013.2258350.

[46] M. S. Moussavi, W. Abdalati, T. Scambos, and A. Neuenschwander, "Applicability of an automatic surface detection approach to micro-pulse photon-counting lidar altimetry data: Implications for canopy height retrieval from future ICESat-2 data," *Int. J. Remote Sens.*, vol. 35, no. 13, pp. 5263–5279, 2014, doi: 10.1080/01431161.2014.939780.

[47] "World Bank Country and Lending Groups." World Bank, 2025. [Online]. Available: https://datahelpdesk.worldbank.org/knowledgebase/articles/906519-world-bank-country-and-lending-groups

[48] I. J. Davenport et al., "First evidence of peat domes in the Congo Basin using LiDAR from a fixed-wing drone," *Remote Sens.*, vol. 12, no. 14, 2020, Art. no. 2196, doi: 10.3390/rs12142196.

[49] A. E. L. Stovall et al., "Comprehensive comparison of airborne and spaceborne SAR and LiDAR estimates of forest structure in the tallest mangrove forest on earth," *Sci. Remote Sens.*, vol. 4, Dec. 2021, Art. no. 100034, doi: 10.1016/j.srs.2021.100034.

[50] Z. Liu et al., "Simultaneous estimation of subcanopy topography and forest height with single-baseline single-polarization TanDEM-X interferometric data combined with ICESat-2 data," *IEEE J. Sel. Topics Appl. Earth Observ. Remote Sens.*, vol. 17, pp. 11,598–11,617, 2024, doi: 10.1109/JSTARS.2024.3410027.

[51] J. Yu et al., "Estimation of forest canopy cover by combining ICESat-2/ATLAS data and geostatistical method/co-kriging," *IEEE J. Sel. Topics Appl. Earth Observ. Remote Sens.*, vol. 17, pp. 1824–1838, 2024, doi: 10.1109/JSTARS.2023.3340429.

[52] D. M. Olson et al., "Terrestrial ecoregions of the world: A new map of life on Earth A new global map of terrestrial ecoregions provides an innovative tool for conserving biodiversity," *BioScience*, vol. 51, no. 11, pp. 933–938, 2001.

[53] F. Jiang, F. Zhao, K. Ma, D. Li, and H. Sun, "Mapping the forest canopy height in Northern China by synergizing ICESat-2 with Sentinel-2 using a stacking algorithm," *Remote Sens.*, vol. 13, no. 8, 2021, Art. no. 1535, doi: 10.3390/rs13081535.

[54] S. C. Popescu et al., "Photon counting LiDAR: An adaptive ground and canopy height retrieval algorithm for ICESat-2 data," *Remote Sens. Environ.*, vol. 208, pp. 154–170, Apr. 2018, doi: 10.1016/j.rse.2018.02.019.

[55] Z. Xi, H. Xu, Y. Xing, W. Gong, G. Chen, and S. Yang, "Forest canopy height mapping by synergizing ICESat-2, Sentinel-1, Sentinel-2 and topographic information based on machine learning methods," *Remote Sens.*, vol. 14, no. 2, 2022, Art. no. 364, doi: 10.3390/rs14020364.

[56] J. C. Fernandez-Diaz, M. Velikova, and C. L. Glennie, "Validation of ICESat-2 ATL08 terrain and canopy height retrievals in tropical mesoamerican forests," *IEEE J. Sel. Topics Appl. Earth Observ. Remote Sens.*, vol. 15, pp. 2956–2970, 2022, doi: 10.1109/JSTARS.2022.3163208.

[57] J. Zang, W. Ni, and Y. Zhang, "Spatially-explicit mapping annual oil palm heights in peninsular Malaysia combining ICESat-2 and stand age data," *Remote Sens. Environ.*, vol. 295, Sep. 2023, Art. no. 113693, doi: 10.1016/j.rse.2023.113693.

[58] M. Liu and S. Popescu, "Estimation of biomass burning emissions by integrating ICESat-2, Landsat 8, and Sentinel-1 data," *Remote Sens. Environ.*, vol. 280, Oct. 2022, Art. no. 113172, doi: 10.1016/j.rse.2022.113172.

[59] L. Narine, L. Malambo, and S. Popescu, "Characterizing canopy cover with ICESat-2: A case study of southern forests in Texas and Alabama, USA," *Remote Sens. Environ.*, vol. 281, Nov. 2022, Art. no. 113242, doi: 10.1016/j.rse.2022.113242.

[60] L. L. Narine, S. Popescu, T. Zhou, S. Srinivasan, and K. Harbeck, "Mapping forest aboveground biomass with a simulated ICESat-2 vegetation canopy product and Landsat data," *Ann. For. Res*, vol. 62, no. 1, pp. 69–86, 2019, doi: 10.15287/afr.2018.1163.

[61] H. Travers-Smith, N. C. Coops, C. Mulverhill, M. A. Wulder, D. Ignace, and T. C. Lantz, "Mapping vegetation height and

identifying the northern forest limit across Canada using ICESat-2, Landsat time series and topographic data," *Remote Sens. Environ.*, vol. 305, May 2024, Art. no. 114097, doi: 10.1016/J.RSE.2024.114097.
[62] Z. Wu and F. Shi, "Mapping forest canopy height at large scales using ICESat-2 and Landsat: An ecological zoning random forest approach," *IEEE Trans. Geosci. Remote Sens.*, vol. 61, pp. 1–16, 2023, doi: 10.1109/TGRS.2022.3231926.
[63] X. Tian and J. Shan, "Comprehensive evaluation of the ICESat-2 ATL08 terrain product," *IEEE Trans. Geosci. Remote Sens.*, vol. 59, no. 10, pp. 8195–8209, Oct. 2021, doi: 10.1109/TGRS.2021.3051086.
[64] J. Zhu, P. f Yang, Y. Li, Y. Zhou Xie, and H. q Fu, "Accuracy assessment of ICESat-2 ATL08 terrain estimates: A case study in Spain," *J. Central South Univ.*, vol. 29, no. 1, pp. 226–238, 2022, doi: 10.1007/S11771-022-4896-X/METRICS.
[65] Y. Wu, R. Zhao, Q. Hu, Y. Zhang, and K. Zhang, "Retrieving sub-canopy terrain from ICESat-2 data based on the RNR-DCM filtering and erroneous ground photons correction approach," *Remote Sens.*, vol. 15, no. 15, 2023, Art. no. 3904, doi: 10.3390/rs15153904.
[66] J. Huang, Y. Xing, Y. Shuai, and H. Zhu, "A novel noise filtering evaluation criterion of ICESat-2 signal photon data in forest environments," *IEEE Geosci. Remote Sens. Lett.*, vol. 19, pp. 1–5, 2022, doi: 10.1109/LGRS.2022.3163143.
[67] D. Guo et al., "Exploring photon-counting laser altimeter ICESat-2 in retrieving LAI and correcting clumping effect," *IEEE Trans. Geosci. Remote Sens.*, vol. 61, pp. 1–9, 2023, doi: 10.1109/TGRS.2022.3233037.
[68] M. Purslow, S. Hancock, A. Neuenschwander, J. Armston, and L. Duncanson, "Can ICESat-2 estimate stand-level plant structural traits? Validation of an ICESat-2 simulator," *Sci. Remote Sens.*, vol. 7, Jun. 2023, Art. no. 100086, doi: 10.1016/j.srs.2023.100086.
[69] J. Zhang et al., "Leaf area index retrieval with ICESat-2 photon counting LiDAR," *Int. J. Appl. Earth Obs. Geoinf.*, vol. 103, Dec. 2021, Art. no. 102488, doi: 10.1016/j.jag.2021.102488.
[70] A. L. Neuenschwander and L. A. Magruder, "The potential impact of vertical sampling uncertainty on ICESat-2/ATLAS terrain and canopy height retrievals for multiple ecosystems," *Remote Sens.*, vol. 8, no. 12, 2016, Art. no. 1039, doi: 10.3390/rs8121039.
[71] F. Cheng, R. Yang, and J. Wu, "Integrating active and passive remote sensing data for forest age estimation in Shangri-La City, China," *Forests*, vol. 15, no. 9, 2024, Art. no. 1622, doi: 10.3390/F15091622/S1.
[72] N. D. Doyog and C. Lin, "Generating wall-to-wall canopy height information from discrete data provided by spaceborne LiDAR system," *Forests*, vol. 15, no. 3, 2024, Art. no. 482, doi: 10.3390/f15030482.
[73] H. Song, L. Xi, Q. Shu, Z. Wei, and S. Qiu, "Estimate forest aboveground biomass of mountain by ICESat-2/ATLAS data interacting cokriging," *Forests*, vol. 14, no. 1, 2023, Art. no. 13, doi: 10.3390/f14010013.
[74] J. Pan et al., "Land cover classification using ICESat-2 photon counting data and Landsat 8 OLI data: A case study in Yunnan Province, China," *IEEE Geosci. Remote Sens. Lett.*, vol. 19, pp. 1–5, 2022, doi: 10.1109/LGRS.2022.3209725.
[75] J. Yang, H. Zheng, Y. Ma, X. Liu, and S. Li, "Instrument radiometric correction of laser signals and background noise for ICESat-2 photon-counting Lidar," *IEEE Geosci. Remote Sens. Lett.*, vol. 21, pp. 1–5, 2024, doi: 10.1109/LGRS.2024.3432732.
[76] J. Yu et al., "Accuracy assessment of ICESat-2 ground elevation and canopy height estimates in mangroves," *IEEE Geosci. Remote Sens. Lett.*, vol. 19, pp. 1–5, 2022, doi: 10.1109/LGRS.2021.3107440.
[77] P. Yang, H. Fu, J. Zhu, Y. Li, and C. Wang, "An elliptical distance based photon point cloud filtering method in forest area," *IEEE Geosci. Remote Sens. Lett.*, vol. 19, pp. 1–5, 2022, doi: 10.1109/LGRS.2021.3124612.
[78] D. Wang, J. Yu, F. Liu, and Q. Li, "ICESat-2 single photon laser point cloud denoising algorithm based on improved DBSCAN clustering," *Earth Planets Space*, vol. 76, no. 1, 2024, Art. no. 128, doi: 10.1186/s40623-024-02071-y.
[79] X. Zhang, S. Xing, Q. Xu, G. Zhang, P. Li, and K. Chen, "Satellite remote sensing image stereoscopic positioning accuracy promotion based on joint block adjustment with ICESat-2 laser altimetry data," *IEEE Access*, vol. 9, pp. 113,362–113,376, 2021, doi: 10.1109/ACCESS.2021.3104302.
[80] X. Zhu et al., "Estimating terrain slope from ICESat-2 data in forest environments," *Remote Sens.*, vol. 12, no. 20, 2020, Art. no. 3300, doi: 10.3390/rs12203300.
[81] J. Lao et al., "Retrieving building height in urban areas using ICESat-2 photon-counting LiDAR data," *Int. J. Appl. Earth Obs. Geoinf.*, vol. 104, Dec. 2021, Art. no. 102596, doi: 10.1016/j.jag.2021.102596.
[82] X. Huang, F. Cheng, J. Wang, B. Yi, and Y. Bao, "Comparative study on remote sensing methods for forest height mapping in complex mountainous environments," *Remote Sens.*, vol. 15, no. 9, 2023, Art. no. 2275, doi: 10.3390/rs15092275.
[83] M. Celesti, M. Rast, J. Adams, V. Boccia, F. Gascon, and C. Isola, "The Copernicus Hyperspectral Imaging Mission for the Environment (CHIME): Status and planning," in *Proc. IEEE Int. Geosci. Remote Sens. Symp. (IGARSS)*, 2022, pp. 5011–5014, doi: 10.1109/IGARSS46834.2022.9883592.
[84] M. Gao, S. Xing, G. Zhang, X. Zhang, and P. Li, "Assessment of ICESat-2's horizontal accuracy using an iterative matching method based on high-accuracy terrains," *Remote Sens.*, vol. 15, no. 9, 2023, Art. no. 2236, doi: 10.3390/rs15092236.
[85] S. Franks and R. Rengarajan, "Evaluation of Copernicus DEM and comparison to the DEM used for Landsat collection-2 processing," *Remote Sens.*, vol. 15, no. 10, 2023, Art. no. 2509, doi: 10.3390/rs15102509.
[86] B. Li et al., "A high-quality global elevation control point dataset from ICESat-2 altimeter data," *Int. J. Digital Earth*, vol. 17, no. 1, 2024, Art. no. 2361724, doi: 10.1080/17538947.2024.2361724.
[87] O. G. Narin and M. Gullu, "A comparison of vertical accuracy of global DEMs and DEMs produced by GEDI, ICESat-2," *Earth Sci. Inf.*, vol. 16, no. 3, pp. 2693–2707, 2023, doi: 10.1007/s12145-023-01060-1.

[88] H. Hu, J. Zhu, H. Fu, Z. Liu, Y. Xie, and K. Liu, "Automated estimation of sub-canopy topography combined with single-baseline single-polarization TanDEM-X InSAR and ICESat-2 data," *Remote Sens.*, vol. 16, no. 7, 2024, Art. no. 1155, doi: 10.3390/rs16071155.

[89] L. Ma et al., "Global evaluation of the Ecosystem Demography model (ED v3.0)," *Geosci. Model Dev.*, vol. 15, no. 5, pp. 1971–1994, 2022, doi: 10.5194/gmd-15-1971-2022.

[90] J. Yu et al., "Mapping global mangrove canopy height by integrating Ice, Cloud, and Land Elevation Satellite-2 photon-counting LiDAR data with multi-source images," *Sci. Total Environ.*, vol. 939, Aug. 2024, Art. no. 173487, doi: 10.1016/j.scitotenv.2024.173487.

[91] T. Zhang and D. Liu, "Improving ICESat-2-based boreal forest height estimation by a multivariate sample quality control approach," *Methods Ecol. Evol.*, vol. 14, no. 7, pp. 1623–1638, 2023, doi: 10.1111/2041-210X.14112.

[92] S. R. Rodda, R. R. Nidamanuri, R. Fararoda, T. Mayamanikandan, and G. Rajashekar, "Evaluation of height metrics and above-ground biomass density from GEDI and ICESat-2 over Indian tropical dry forests using airborne LiDAR data," *J. Indian Soc. Remote Sens.*, vol. 52, no. 4, pp. 841–856, 2024, doi: 10.1007/s12524-023-01693-1.

[93] C. Mulverhill, N. C. Coops, T. Hermosilla, J. C. White, and M. A. Wulder, "Evaluating ICESat-2 for monitoring, modeling, and update of large area forest canopy height products," *Remote Sens. Environ.*, vol. 271, Mar. 2022, Art. no. 112919, doi: 10.1016/j.rse.2022.112919.

[94] M. Santoro et al., "Design and performance of the Climate Change Initiative Biomass global retrieval algorithm," *Sci. Remote Sens.*, vol. 10, Dec. 2024, Art. no. 100169, doi: 10.1016/j.srs.2024.100169.

[95] M. Milenković et al., "Assessing Amazon rainforest regrowth with GEDI and ICESat-2 data," *Sci. Remote Sens.*, vol. 5, Jun. 2022, Art. no. 100051, doi: 10.1016/j.srs.2022.100051.

[96] L. Ma et al., "Spatial heterogeneity of global forest aboveground carbon stocks and fluxes constrained by spaceborne lidar data and mechanistic modeling," *Global Change Biol.*, vol. 29, no. 12, pp. 3378–3394, 2023, doi: 10.1111/gcb.16682.

[97] A. Neuenschwander et al., "Towards global spaceborne lidar biomass: Developing and applying boreal forest biomass models for ICESat-2 laser altimetry data," *Sci. Remote Sens.*, vol. 10, Dec. 2024, Art. no. 100150, doi: 10.1016/j.srs.2024.100150.

[98] S. Nandy, R. Srinet, and H. Padalia, "Mapping forest height and aboveground biomass by integrating ICESat-2, Sentinel-1 and Sentinel-2 data using random forest algorithm in northwest Himalayan foothills of India," *Geophys. Res. Lett.*, vol. 48, no. 14, 2021, Art. no. e2021GL093799, doi: 10.1029/2021GL093799.

[99] Z. Qin et al., "Estimation of Leaf Area Index for Dendrocalamus giganteus based on multi-source remote sensing data," *Forests*, vol. 15, no. 7, 2024, Art. no. 1257, doi: 10.3390/f15071257.

[100] Y. Wang and H. Fang, "Derivation and evaluation of LAI from the ICESat-2 data over the NEON sites: The impact of segment size and beam type," *Remote Sens.*, vol. 16, no. 16, 2024, Art. no. 3078, doi: 10.3390/rs16163078.

[101] Z. Yang, Q. Shu, L. Zhang, and X. Yang, "Forest tree species diversity mapping using ICESat-2/ATLAS with GF-1/PMS imagery," *Forests*, vol. 14, no. 8, 2023, Art. no. 1537, doi: 10.3390/f14081537.

[102] T. Chen, J. Wang, T. Che, X. Hao, and H. Li, "High spatial resolution elevation change dataset derived from ICESat-2 crossover points on the Tibetan Plateau," *Sci. Data*, vol. 11, no. 1, 2024, Art. no. 394, doi: 10.1038/s41597-024-03214-2.

[103] M. Agca et al., "Machine learning algorithms for building height estimations using ICESat-2/ATLAS and Airborne LiDAR data," *Earth Sci. Inf.*, vol. 17, no. 6, pp. 5123–5134, 2024, doi: 10.1007/S12145-024-01429-W/FIGURES/8.

[104] Q. Zhang, H. Zhou, Y. Ma, H. Wang, S. Li, and Y. Chen, "ICESat-2 derived canopy covers with radiometric and reflectance ratio corrections," *IEEE Trans. Geosci. Remote Sens.*, vol. 62, pp. 1–14, 2024, doi: 10.1109/TGRS.2024.3349559.

[105] J. Yu, L. Xu, Q. Shu, S. Luo, and L. Xi, "Spatial effects analysis of natural forest canopy cover based on spaceborne LiDAR and geostatistics," *Front. Plant Sci.*, vol. 15, Jul. 2024, Art. no. 1361297, doi: 10.3389/FPLS.2024.1361297/BIBTEX.

[106] L. L. Narine, S. Popescu, A. Neuenschwander, T. Zhou, S. Srinivasan, and K. Harbeck, "Estimating aboveground biomass and forest canopy cover with simulated ICESat-2 data," *Remote Sens. Environ.*, vol. 224, pp. 1–11, Apr. 2019, doi: 10.1016/j.rse.2019.01.037.

[107] L. Malambo and S. Popescu, "Mapping vegetation canopy height across the contiguous United States using ICESat-2 and ancillary datasets," *Remote Sens. Environ.*, vol. 309, Aug. 2024, Art. no. 114226, doi: 10.1016/J.RSE.2024.114226.

[108] J. Guerra-Hernández et al., "Aboveground biomass mapping by integrating ICESat-2, SENTINEL-1, SENTINEL-2, ALOS2/PALSAR2, and topographic information in Mediterranean forests," *GISci. Remote Sens.*, vol. 59, no. 1, pp. 1509–1533, 2022, doi: 10.1080/15481603.2022.2115599.

[109] X. Wang, X. Liang, W. Gong, P. Häkli, and Y. Wang, "Accuracy fluctuations of ICESat-2 height measurements in time series," *Int. J. Appl. Earth Obs. Geoinf.*, vol. 135, Dec. 2024, Art. no. 104234, doi: 10.1016/j.jag.2024.104234.

[110] G. Li et al., "Stepwise estimation of height change time series and two-dimensional surface deformation over mountain excavation and City construction region with TS-InSAR technique," *Int. J. Appl. Earth Obs. Geoinf.*, vol. 131, Jul. 2024, Art. no. 103982, doi: 10.1016/J.JAG.2024.103982.

[111] Q. Yu et al., "Assessing canopy height measurements from ICESat-2 and GEDI orbiting LiDAR across six different biomes with G-LiHT LiDAR," *Environ. Res. Ecol.*, vol. 3, no. 2, 2024, Art. no. 025001, doi: 10.1088/2752-664X/ad39f2.

[112] C. Vatandaslar, O. G. Narin, and S. Abdikan, "Retrieval of forest height information using spaceborne LiDAR data: A comparison of GEDI and ICESat-2 missions for Crimean pine (Pinus nigra) stands," *Trees*, vol. 37, no. 3, pp. 717–731, 2023, doi: 10.1007/s00468-022-02378-x.

[113] X. Liu et al., "Neural network guided interpolation for mapping canopy height of China's forests by integrating GEDI and ICESat-2 data," *Remote Sens. Environ.*, vol. 269, Feb. 2022, Art. no. 112844, doi: 10.1016/j.rse.2021.112844.

[114] Z. Wu, F. Yao, J. Zhang, E. Ma, L. Yao, and Z. Dong, "Genetic programming guided mapping of forest canopy height by combining LiDAR satellites with Sentinel-1/2, terrain, and climate data," *Remote Sens.*, vol. 16, no. 1, 2023, Art. no. 110, doi: 10.3390/rs16010110.

[115] L. L. Narine, S. C. Popescu, and L. Malambo, "A methodological framework for mapping canopy cover using ICESat-2 in the Southern USA," *Remote Sens.*, vol. 15, no. 6, 2023, Art. no. 1548, doi: 10.3390/rs15061548.

[116] B. Li, H. Xie, X. Tong, H. Tang, and S. Liu, "A global-scale DEM elevation correction model using ICESat-2 laser altimetry data," *IEEE Trans. Geosci. Remote Sens.*, vol. 61, pp. 1–15, 2023, doi: 10.1109/TGRS.2023.3321956.

[117] E. Akturk, S. C. Popescu, and L. Malambo, "ICESat-2 for canopy cover estimation at large-scale on a cloud-based platform," *Sensors*, vol. 23, no. 7, 2023, Art. no. 3394, doi: 10.3390/s23073394.

[118] Y. Li, H. Fu, S. Gao, J. Zhu, L. Wang, and C. Wang, "Retrieving low and sparse vegetation heights in desert ecosystems using ICESat-2 ATL03 photon-counting LiDAR data," *IEEE Geosci. Remote Sens. Lett.*, vol. 19, pp. 1–5, 2022, doi: 10.1109/LGRS.2022.3194877.

[119] R. Wang, Y. Lu, D. Lu, and G. Li, "Improving extraction of forest canopy height through reprocessing ICESat-2 ATLAS and GEDI data in sparsely forested plain regions," *GISci. Remote Sens.*, vol. 61, no. 1, 2024, Art. no. 2396807, doi: 10.1080/15481603.2024.2396807.

[120] V. Moudrý et al., "Effects of environmental conditions on ICESat-2 terrain and canopy heights retrievals in Central European mountains," *Remote Sens. Environ.*, vol. 279, Sep. 2022, Art. no. 113112, doi: 10.1016/J.RSE.2022.113112.

[121] E. N. Stavros et al., "ISS observations offer insights into plant function," *Nature Ecol. Evol.*, vol. 1, no. 7, 2017, Art. no. 0194, doi: 10.1038/s41559-017-0194.

[122] M. Liu, S. Popescu, and L. Malambo, "Effects of spatial resolution on burned forest classification with ICESat-2 photon counting data," *Frontiers Remote Sens.*, vol. 2, Jul. 2021, Art. no. 666251, doi: 10.3389/frsen.2021.666251.

[123] X. Zhu, S. Nie, C. Wang, X. Xi, J. Lao, and D. Li, "Consistency analysis of forest height retrievals between GEDI and ICESat-2," *Remote Sens. Environ.*, vol. 281, Nov. 2022, Art. no. 113244, doi: 10.1016/j.rse.2022.113244.

[124] S. Saarela et al., "Three-phase hierarchical model-based and hybrid inference," *MethodsX*, vol. 11, Dec. 2023, Art. no. 102321, doi: 10.1016/j.mex.2023.102321.

[125] S. Pang, G. Li, X. Jiang, Y. Chen, Y. Lu, and D. Lu, "Retrieval of forest canopy height in a mountainous region with ICESat-2 ATLAS," *Forest Ecosystems*, vol. 9, Jan. 2022, Art. no. 100046, doi: 10.1016/j.fecs.2022.100046.

[126] G. Yin et al., "Adaptive OPTICS algorithm denoising ICESat-2 laser photon data," *IEEE Geosci. Remote Sens. Lett.*, vol. 21, pp. 1–5, 2024, doi: 10.1109/LGRS.2024.3449446.

[127] J. Tang et al., "A multilevel autoadaptive denoising algorithm based on forested terrain slope for ICESat-2 photon-counting data," *IEEE J. Sel. Topics Appl. Earth Observ. Remote Sens.*, vol. 17, pp. 16,831–16,846, 2024, doi: 10.1109/JSTARS.2024.3459957.

[128] W. Qin, Y. Song, Y. Zou, H. Zhu, and H. Guan, "A novel ICESat-2 signal photon extraction method based on convolutional neural network," *Remote Sens.*, vol. 16, no. 1, 2024, Art. no. 203, doi: 10.3390/rs16010203.

[129] J. Pan, F. Gao, J. Wang, J. Zhang, Q. Liu, and Y. Deng, "A main direction-based noise removal algorithm for ICESat-2 photon-counting LiDAR data," *J. Geod.*, vol. 98, no. 9, pp. 1–23, 2024, doi: 10.1007/S00190-024-01887-6/FIGURES/14.

[130] J. Huang and T. Xia, "Multilevel adaptive photon cloud noise filtering algorithm for different observation time scenes in forest environments," *IEEE Trans. Geosci. Remote Sens.*, vol. 62, pp. 1–16, 2024, doi: 10.1109/TGRS.2023.3347401.

[131] G. He, H. Wang, D. Zhao, Q. Fang, and Y. Zhang, "Extraction of ground photon for photon counting lidar over rugged mountainous area based on wavelet transform with adaptive window," *IEEE Geosci. Remote Sens. Lett.*, vol. 21, pp. 1–5, 2024, doi: 10.1109/LGRS.2023.3344873.

[132] S. Chen et al., "A novel multidimensional statistics denoising algorithm based on gaussian mixture model for photon-counting LiDAR data," *IEEE J. Sel. Topics Appl. Earth Observ. Remote Sens.*, vol. 17, pp. 13,308–13,323, 2024, doi: 10.1109/JSTARS.2024.3430470.

[133] X. Huang et al., "Urban building height extraction accommodating various terrain scenes using ICESat-2/ATLAS data," *Int. J. Appl. Earth Obs. Geoinf.*, vol. 130, Jun. 2024, Art. no. 103870, doi: 10.1016/J.JAG.2024.103870.

[134] D. P. Duda, J. D. Spinhirne, and E. W. Eloranta, "Atmospheric multiple scattering effects on GLAS altimetry. I. Calculations of single pulse bias," *IEEE Trans. Geosci. Remote Sens.*, vol. 39, no. 1, pp. 92–101, Jan. 2001, doi: 10.1109/36.898668.

[135] S. Palm, Y. Yang, U. Herzfeld, and D. Hancock, "ICE, CLOUD, and Land Elevation Satellite (ICESat-2) project: Algorithm theoretical basis document for the atmosphere, Part I: Level 2 and 3 data products, version 6. ICESat-2 project," 2022.

[136] B. Li, H. Xie, S. Liu, X. Tong, H. Tang, and X. Wang, "A method of extracting high-accuracy elevation control points from ICESat-2 altimetry data," *Photogramm. Eng. Remote Sens.*, vol. 87, no. 11, pp. 821–830, 2021, doi: 10.14358/PERS.21-00009R2.

[137] M. Queinnec, J. C. White, and N. C. Coops, "Comparing airborne and spaceborne photon-counting LiDAR canopy structural estimates across different boreal forest types," *Remote Sens. Environ.*, vol. 262, Sep. 2021, Art. no. 112510, doi: 10.1016/j.rse.2021.112510.

[138] S. Palm, Y. Yang, U. Herzfeld, and D. Hancock, "The atmospheric measurements of ICESat-2," presented at the Amer. Meteorol. Soc. Annu. Meeting, Boston, MA, USA, Jan. 12–16, 2020.

[139] M. Queinnec, N. C. Coops, and J. C. White, "Characterizing post-fire northern boreal forest height dynamics," *Int. J. Remote Sens.*, vol. 45, no. 7, pp. 2182–2207, 2024, doi: 10.1080/01431161.2024.2326534.

[140] P. Varvia et al., “Estimation of boreal forest biomass from ICESat-2 data using hierarchical hybrid inference,” *Remote Sens. Environ.*, vol. 311, Sep. 2024, Art. no. 114249, doi: 10.1016/J.RSE.2024.114249.

[141] Y. Li, J. Zhu, H. Fu, S. Gao, and C. Wang, “Filtering photon cloud data in forested areas based on elliptical distance parameters and machine learning approach,” *Forests*, vol. 13, no. 5, 2022, Art. no. 663, doi: 10.3390/f13050663.

[142] D. Gwenzi, M. A. Lefsky, V. P. Suchdeo, and D. J. Harding, “Prospects of the ICESat-2 laser altimetry mission for savanna ecosystem structural studies based on airborne simulation data,” *ISPRS J. Photogramm. Remote Sens.*, vol. 118, pp. 68–82, Aug. 2016, doi: 10.1016/j.isprsjprs.2016.04.009.

[143] R. O. Dubayah, S. B. Luthcke, T. J. Sabaka, J. B. Nicholas, S. Preaux, and M. A. Hofton, 2021, “GEDI L3 Gridded Land Surface Metrics, Version 2,” NASA Open Data Portal. [Online]. Available: https://data.nasa.gov/dataset/gedi-l3-gridded-land-surface-metrics-version-2-73ff2

[144] P. Burns et al., “Incorporating canopy structure from simulated GEDI lidar into bird species distribution models,” *Environ. Res. Lett.*, vol. 15, no. 9, 2020, Art. no. 095002, doi: 10.1088/1748-9326/ab80ee.

[145] J. Liu, J. Heiskanen, E. E. Maeda, and P. K. E. Pellikka, “Burned area detection based on Landsat time series in savannas of southern Burkina Faso,” *Int. J. Appl. Earth Obs. Geoinf.*, vol. 64, pp. 210–220, Feb. 2018, doi: 10.1016/j.jag.2017.09.011.

[146] R. V. Leite et al., “Leveraging the next generation of spaceborne Earth observations for fuel monitoring and wildland fire management,” *Remote Sens. Ecology Conservation*, vol. 11, no. 2, pp. 133–155, 2024, doi: 10.1002/rse2.416.

[147] Y. Zhao et al., “Combining ICESat-2 photons and Google Earth Satellite images for building height extraction,” *Int. J. Appl. Earth Obs. Geoinf.*, vol. 117, Mar. 2023, Art. no. 103213, doi: 10.1016/j.jag.2023.103213.

[148] B. Li, H. Xie, S. Liu, Y. Sun, Q. Xu, and X. Tong, “Correction of ICESat-2 terrain within urban areas using a water pump deployment criterion with the vertical contour of the terrain,” *Remote Sens. Environ.*, vol. 298, Dec. 2023, Art. no. 113817, doi: 10.1016/J.RSE.2023.113817.

[149] C. S. Watson, J. R. Elliott, R. M. J. Amey, and K. E. Abdrakhmatov, “Analyzing satellite-derived 3D building inventories and quantifying urban growth towards active faults: A case study of Bishkek, Kyrgyzstan,” *Remote Sens.*, vol. 14, no. 22, 2022, Art. no. 5790, doi: 10.3390/RS14225790/S1.

[150] T. Sun, J. Qi, and H. Huang, “Discovering forest height changes based on spaceborne lidar data of ICESat-1 in 2005 and ICESat-2 in 2019: A case study in the Beijing-Tianjin-Hebei region of China,” *Forest Ecosystems*, vol. 7, no. 1, 2020, Art. no. 53, doi: 10.1186/s40663-020-00265-w.

[151] A. Stritih, C. Senf, T. Marsoner, and R. Seidl, “Mapping the natural disturbance risk to protective forests across the European Alps,” *J. Environ. Manage.*, vol. 366, Aug. 2024, Art. no. 121659, doi: 10.1016/j.jenvman.2024.121659.

[152] D. Rocchini et al., “Measuring β-diversity by remote sensing: A challenge for biodiversity monitoring,” *Methods Ecol. Evol*, vol. 9, no. 8, pp. 1787–1798, 2018, doi: 10.1111/2041-210X.12941.

[153] D. Rocchini, M. Torresani, and C. Ricotta, “On the mathematical properties of spatial Rao’s Q to compute ecosystem heterogeneity,” *Theor. Ecol.*, vol. 17, no. 3, pp. 247–254, 2024, doi: 10.1007/s12080-024-00587-3.

[154] N. K. Corak, J. A. Otkin, T. W. Ford, and L. E. L. Lowman, “Unraveling phenological and stomatal responses to flash drought and implications for water and carbon budgets,” *Hydrol. Earth Syst. Sci.*, vol. 28, no. 8, pp. 1827–1851, 2024, doi: 10.5194/hess-28-1827-2024.

[155] M. Liu, S. Popescu, and L. Malambo, “Feasibility of burned area mapping based on ICESAT-2 photon counting data,” *Remote Sens.*, vol. 12, no. 1, 2019, Art. no. 24, doi: 10.3390/RS12010024.

[156] N. F. Glenn et al., “Landsat 8 and ICESat-2: Performance and potential synergies for quantifying dryland ecosystem vegetation cover and biomass,” *Remote Sens. Environ.*, vol. 185, pp. 233–242, Nov. 2016, doi: 10.1016/j.rse.2016.02.039.

[157] L. J. Hamberg, J. B. Fisher, J. L. W. Ruppert, J. Tureček, D. H. Rosen, and P. M. A. James, “Assessing and modeling diurnal temperature buffering and evapotranspiration dynamics in forest restoration using ECOSTRESS thermal imaging,” *Remote Sens. Environ.*, vol. 280, Oct. 2022, Art. no. 113178, doi: 10.1016/j.rse.2022.113178.

[158] A. Valdés-Uribe, D. Hölscher, and A. Röll, “ECOSTRESS Reveals the Importance of Topography and Forest Structure for Evapotranspiration from a Tropical Forest Region of the Andes,” *Remote Sens.*, vol. 15, no. 12, 2023, Art. no. 2985, doi: 10.3390/rs15122985.

[159] M. J. Soja et al., “Design and parameter estimation robustness of the global above-ground biomass estimation algorithm for ESA’s 7th Earth Explorer Mission Biomass,” in *Proc. IEEE Int. Geosci. Remote Sens. Symp. (IGARSS)*, 2023, pp. 1756–1759, doi: 10.1109/IGARSS52108.2023.10282791.

[160] E. N. Stavros et al., “Designing an observing system to study the Surface Biology and Geology (SBG) of the Earth in the 2020s,” *J. Geophys. Res. Biogeosci.*, vol. 128, no. 1, 2023, Art. no. e2021JG006471, doi: 10.1029/2021JG006471.

[161] K. R. Turpie et al., “Calibration and validation for the Surface Biology and Geology (SBG) Mission concept: Recommendations for a multi-sensor system for imaging spectroscopy and thermal imagery,” *J. Geophys. Res. Biogeosci.*, vol. 128, no. 9, 2023, Art. no. e2023JG007452, doi: 10.1029/2023JG007452.

GRS